Plant Physiology Preview. Published on June 16, 2015, as DOI:10.1104/pp.15.00736

Integrative comparison of the role of the PHR1 subfamily in phosphate signaling and homeostasis in rice

Meina Guo[1¥], Wenyuan Ruan[2, 1,¥], Changying Li[1], Fangliang Huang[1], Ming Zeng[1], Yingyao Liu[1], Yanan Yu[1], Xiaomeng Ding[1], Yunrong Wu[1], Zhongchang Wu[1], Chuanzao Mao[1], Keke Yi[2, 1], Ping Wu[1], Xiaorong Mo[1]*

Author affiliation:

[1] State Key Laboratory of Plant Physiology and Biochemistry, College of Life Sciences, Zhejiang University, Hangzhou 310058, China.

[2] Institute of Agricultural Resources and Regional Planning, China Academy of Agricultural Sciences, Beijing 100081, China.

[¥] Wenyuan Ruan and Meina Guo contributed equally to this work.

*To whom correspondence should be addressed. E-mail: xiaorong@zju.edu.cn

E-mail of all authors:

Meina Guo (guomeina@zju.edu.cn);

Wenyuan Ruan (ruanwenyuan@zju.edu.cn);

Changying Li (21107015@zju.edu.cn);

Fangliang Huang (huangfl@zju.edu.cn)

Yanan Yu (21207008@zju.edu.cn);

Ming Zeng (21307003@zju.edu.cn);

Yingyao Liu (lyingyao@zju.edu.cn);

Xiaomeng Ding (21307007@zju.edu.cn);

Yunrong Wu (yrwu@zju.edu.cn);

Zhongchang Wu (wzchang@zju.edu.cn);

Chuanzao Mao (mcz@zju.edu.cn) ;

Keke Yi (yikk@zju.edu.cn);

Ping Wu (clspwu@zju.edu.cn)

Xiaorong Mo (xiaorong@zju.edu.cn)

Abstract

Phosphorus (P), an essential macronutrient for all living cells, is indispensable for agricultural production. While *Arabidopsis thaliana* PHOSPHATE RESPONSE1 (PHR1) and its orthologs

in other species have been shown to function in transcriptional regulation of phosphate (Pi) signaling and Pi homeostasis, an integrative comparison of PHR1-related proteins in rice has not previously been reported. Here, we identified functional redundancy among three PHR1 orthologs in rice, OsPHR1, OsPHR2 and OsPHR3, using phylogenetic and mutation analysis. OsPHR3, in conjunction with OsPHR1 and OsPHR2, function in transcriptional activation of most Pi starvation-induced (PSI) genes. Loss-of-function mutations in any one of these transcription factors (TFs) impaired root hair growth (primarily root hair elongation). However, these three TFs showed differences in DNA binding affinities and mRNA expression patterns in different tissues and growth stages, and transcriptomic analysis revealed differential effects on PSI gene expression of single mutants of the three TFs, indicating some degree of functional diversification. Overexpression of genes encoding any of these TFs resulted in partial constitutive activation of Pi starvation response and led to Pi accumulation in the shoot. Furthermore, unlike *OsPHR2*-overexpressing lines, which exhibited growth retardation under normal or Pi-deficient conditions, *OsPHR3*-overexpressing plants exhibited significant tolerance to low Pi stress but normal growth rates under normal Pi conditions, suggesting that *OsPHR3* would be useful for molecular breeding to improve Pi uptake/use efficiency under phosphate-deficient conditions. We propose that OsPHR1, OsPHR2 and OsPHR3 form a network and play diverse roles in regulating Pi signaling and homeostasis in rice.

Key words: Phosphate, PHR transcription factors, Rice, Low phosphate stress

Introduction

Phosphorus (P), an essential macronutrient for all living cells, is a constituent of key molecules such as ATP, nucleic acids and phospholipids (**Rubio et al., 2001; Cheng et al., 2011**). Although the overall P content in soil is high, P represents a limiting factor for plant growth due to its rapid immobilization by soil organic and inorganic components in many natural and agricultural ecosystems (**for review, see Richardson et al., 2009; Rouached et al., 2010; Hinsinger et al., 2011**). Consequently, plants have evolved strategies to cope with a limited phosphate (Pi) supply, including mechanisms to increase Pi uptake and to use and recycle P more efficiently in the plant (**Nilsson et al., 2007**). PHOSPHATE STARVATION RESPONSE1 (PHR1) in *Arabidopsis thaliana* (Arabidopsis) and its orthologs in other species play key roles in these processes by regulating Pi-signaling and Pi-homeostasis to help the plant adapt to Pi deficiency by binding to a *cis*-element with an imperfect palindromic sequence [GnATATnC, i.e., PHR1 binding site (P1BS)] (**Rubio et al., 2001; Bari *et al*., 2006; Zhou et al., 2008; Bustos et al., 2010**). PHR1 functions in three main regulatory pathways, as described below.

The first (and most important) Pi regulatory pathway includes five key members: PHR1, IPS1, miR399, PHO2 and PT. PHR1 directly binds to the promoters of *IPS1* (a non-coding RNA) (**Martín et al., 2000**) and microRNA399 (miR399) under Pi-deficient conditions (**Rubio et al., 2001; Busto et al., 2010, Wang et al., 2014, Lv et al., 2014**). Next, miR399 represses the expression of *PHOSPHATE2* (*PHO2*), encoding an ubiquitin-conjugating E2 enzyme (UBC24), under Pi-starvation conditions (**Bari et al., 2006; Hu et al., 2011**). In addition, *IPS1* can mimic the target of *miR399* to block cleavage of *PHO2* when the Pi supply is limited (**Franco-Zorrilla *et al*., 2007**). Recently, PHO2 was shown to modulate Pi acquisition by regulating the abundance of PHOSPHATE TRANSPORTER1 (PHT1) in the secretory pathway destined for the plasma membrane (**Huang *et al*., 2013**).

The second pathway involves PHR1, miR827, NLA1 and PT. Like *IPS1* and *miR399*, *miR827* is also directly regulated by PHR1 (**Lin *et al*., 2010**). Overexpression of *miR827* leads to accumulation of Pi in shoots (**Wang et al., 2012**) and reduces the mRNA level of *NITROGEN LIMITATION ADAPTATION1* (*NLA1*), which encodes a RING-type ubiquitin E3 ligase (**Hsieh et al., 2009; Kant et al., 2011**). The *nla1* mutant accumulates Pi under nitrogen-deficient conditions (**Peng et al., 2007**). Moreover, NLA1 recruits PHO2 for the degradation of Pi

transporters to help maintain cellular Pi homeostasis (**Lin *et al*., 2013; Park *et al*., 2014**).

The third pathway involves PHR1, PT/PAP or SQD. In this pathway, PHR1 directly binds to its target gene promoters to regulate their expression, thereby enabling the plant to adapt to changes in cellular and environmental phosphate levels. OsPHT1;2 (OsPT2), a low-affinity Pi transporter that functions in the Pi translocation process, directs the expression of downstream targets of OsPHR2 in rice (**Liu et al., 2010**). The expression of *AtPHT1;1* (containing a P1BS motif in its promoter region) is dramatically reduced in the *phr1/phl1* double mutant (**Bustos *et al*., 2010**). Most purple acid phosphatases (PAPs) function in the production and recycling of Pi from organic P (**Tran et al., 2010; Zhang et al., 2011**). *PAP* genes contain P1BS motifs in their promoters, implying that they are direct targets of PHR1 (**Wu et al., 2013**). In addition, the gene encoding sulfoquinovosyl diacylglycerol 2 (SQD2), which functions in recycling Pi from membrane phospholipids, also contains the P1BS motif (**Yu et al., 2002, Wu et al., 2013**).

In addition to functioning in these regulatory pathways, PHR1 takes part in other plant growth and developmental processes. For example, PHR1 regulates shoot-to-root sulfate transport by directly binding to the promoters of sulfate transporter-encoding genes *SULTR1;3* and *SULTR3;4* (**Rouached et al., 2011**). Because the *phr1* mutant is much more sensitive to photochemical stress than the wild type, Nilsson *et al.* (2012) proposed that PHR1 is essential for plant adaptation to high light levels and for maintaining functional photosynthesis during Pi starvation. Arabidopsis FERRITIN 1 (AtFER1) is regulated by AtPHR1, demonstrating a direct molecular link between iron and Pi homeostasis (**Bournier et al., 2013**). The responses to Pi and oxygen deficiency stress were recently shown to both be controlled by PHR1 (**Klecker et al., 2014**).

PHR1 subfamily transcription factors (PHR TFs) are regulated by other factors at the protein level. AtPHR1 is sumoylated by AtSIZ1, a plant small ubiquitin-like modifier (SUMO) E3 ligase that is a primary controller of Pi-starvation-dependent responses (**Miura et al., 2005**). SPX family proteins [named for SYG1 (suppressor of yeast gpa1), Pho81 (CDK inhibitor in yeast PHO pathway) and XPR1 (xenotropic and polytropic retrovirus receptor)] regulate the transcriptional activity and localization of PHRs by directly interacting with these proteins in a Pi-dependent manner (**Lv et al., 2014, Wang et al., 2014; Puga et al., 2014**).

Although the importance of AtPHR1 in Arabidopsis and OsPHR2 in rice in the Pi-starvation response has been described in detail, how different OsPHRs engage in Pi signaling and

115 homeostasis in rice is currently unclear. In this study, we showed that three *OsPHR* genes are
116 functionally redundant in Pi signaling and in determining root hair morphology. Overexpressing
117 any one of these genes led to Pi accumulation in the shoot as well as root hair elongation, which
118 results the Pi-starvation response. Furthermore, the tissue-specific expression patterns and DNA
119 binding affinity differed among OsPHRs. We also highlight the potential of using *OsPHR3* in the
120 molecular breeding of crops, as lines overexpressing this gene were tolerant to low-Pi stress.
121

122

Results

Redundancy of PHR1-PHR3 in the control of Pi starvation responses

Knockdown of *OsPHR1* and *OsPHR2* (*PHR1-Ri* and *PHR2-Ri*) expression leads to various degrees of reduction in Pi-starvation responses, as revealed by the expression of a set of Pi-starvation response genes (**Zhou et al., 2008**). The incomplete impairment of these responses in the knockdown plants could be explained by partial gene redundancy, as OsPHR1 and OsPHR2 belong to a MYB-CC domain-containing transcription factor family with at least four close members in cereal crops (**Figure S1**). To investigate the possibility of partial gene redundancy among these PHR1-related genes, we searched for T-DNA or Tos-17 insertional mutants harboring mutations in *PHR1*-related genes in public databases. A T-DNA insertional mutant with a mutation in *PHR2*, the *phr2* mutant, was previously isolated (**Chen et.al., 2011**). Here, we identified a phylogenetically closely related rice gene, Os02g04640, termed *OsPHR3*, for which the mutant *phr3* was available. OsPHR3 displayed a high degree of amino acid identity to OsPHR1 and OsPHR2, and the Tos-17 insertion disrupted the coding region of *OsPHR3* mRNA (**Figure S2).** Because an *OsPHR1* mutant was not found in the public databases, we created an *OsPHR1* mutant, *phr1,* using the CRISPR/Cas system (**Feng et al., 2013**) system. After characterizing the CRISPR/Cas targeting site, we found a two-base 'AC' deletion at the first exon of *OsPHR1*, leading to *OsPHR1* malfunction (deletion of the 'AC' at 223 nt from the start codon 'ATG') (**Figure S3**).

After generating the homozygous double mutants *phr1/2*, *phr1/3*, and *phr2/3* and the triple mutant *phr1/2/3*, we performed phenotypic and physiological tests on wild-type, *phr1*, *phr2*, *phr3*, *phr1/2*, *phr1/3*, *phr2/3* and *phr1/2/3* plants. Plant growth was retarded in the *phr2* mutant, and additive inhibition of plant growth in *phr1/2*, *phr2/3* and *phr1/2/3* was observed under Pi-sufficient (200 μM Pi) and Pi-deficient (10 μM Pi) conditions (**Figure 1A, B**). The most significant repression of growth occurred in the triple mutant *phr1/2/3*. There was no significant difference in Pi concentration in all single or double mutants compared to wild type (**Figure 1C**), which is different from that of the *phr1* and *phl1* mutants in Arabidopsis (**Rubio et al., 2001; Bustos et al., 2010**). However, for the triple mutant *phr1/2/3*, the Pi concentration was obviously reduced in both shoots and roots compared with wild type (**Figure 1C**).

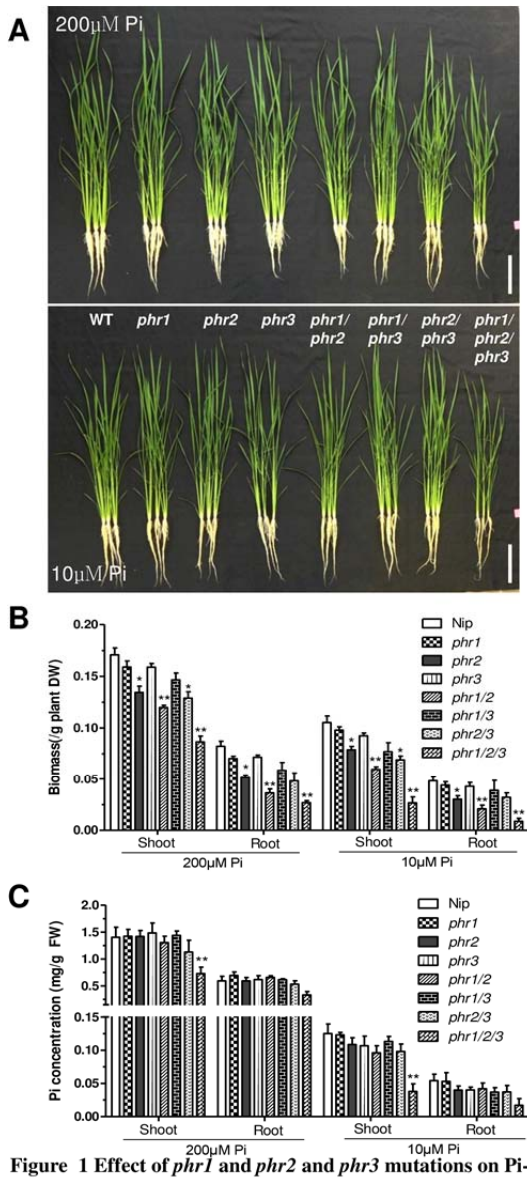

Figure 1 Effect of *phr1* and *phr2* and *phr3* mutations on Pi-homeostasis

A, Phenotypic performance of 30-d-old wild type (WT) plants, *phr1*, *phr2* and *phr3* mutants, *phr1/2, phr1/3* and *phr2/3* double mutants, and *phr1/2/3* triple mutant under Pi-sufficient (200 μM Pi) and Pi-deficient (10 μM Pi) hydroponic conditions. Bars = 10 cm.

B and C, Histograms of dried biomass (B) and cellular Pi concentration (C) of shoots and roots of 30-d-old wild type (WT) plants, *phr1*, *phr2* and *phr3* single mutants, *phr1/2, phr1/3* and *phr2/3* double mutants, and *phr1/2/3* triple mutant under Pi-sufficient (200 μM Pi) and Pi-deficient (10 μM Pi) conditions. Values represent means ± standard deviation (SD) of three replicates. Data significantly different from the corresponding controls are indicated (*phr1*, *phr2* and *phr3* mutant versus wt, $*P < 0.05$; *phr1/2*, *phr1/3*, *phr2/3* double mutants, and *phr1/2/3* plants versus other plants, $**P < 0.01$; Student's *t*-test).

A previous study demonstrated that overexpressing *OsPHR2* induces results in Pi accumulation in shoots under Pi-sufficient conditions (**Zhou et al., 2008**). We therefore constructed transgenic plants overexpressing *OsPHR3* and analyzed Pi concentrations in these

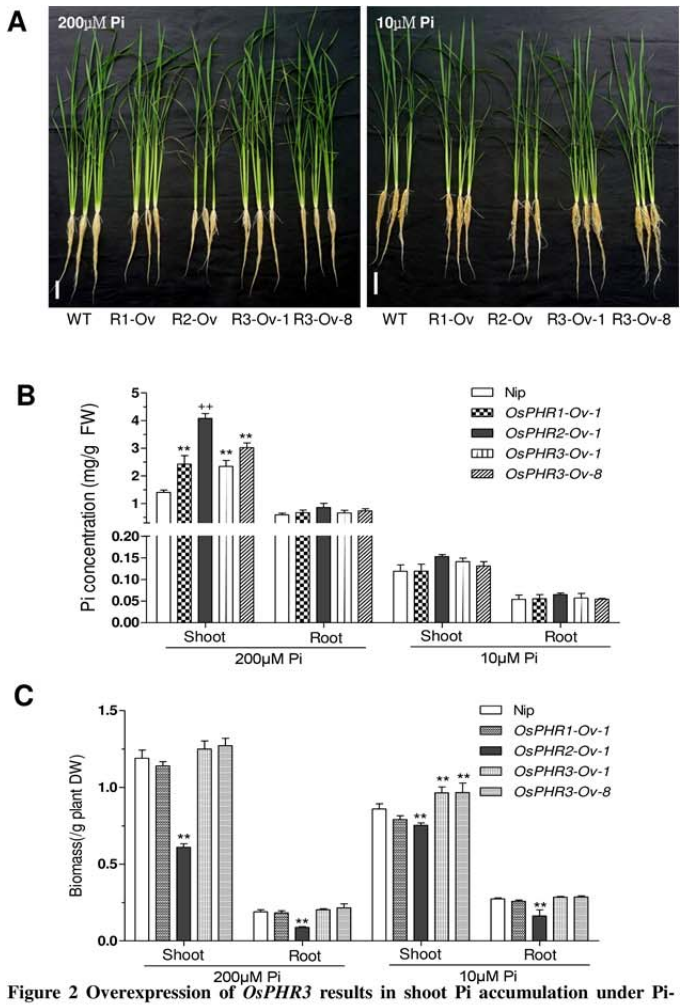

Figure 2 Overexpression of *OsPHR3* results in shoot Pi accumulation under Pi-sufficient conditions, like as *OsPHR1* and *OsPHR2*

A, Phenotypic performance of two independent *OsPHR3*-overexpressing plants (*OsPHR3-Ov1* and *OsPHR3-Ov8*) compared to wild type (WT) and *PHR1/2*-overexpressing plants (Zhou et.al, 2008) under Pi-sufficient (200 μM Pi) and Pi-deficient (10 μM Pi) conditions. Two independent lines of *OsPHR3* overexpressors were confirmed by DNA gel blot analysis (**See Figure S3**). Bars = 10 cm.

B, Cellular Pi levels in shoots and roots of 30-d-old WT and *PHR1-3*-overexpressing plants grown in hydroponic culture under Pi-sufficient and Pi-deficient conditions. Data significantly different from corresponding controls are indicated (overexpressing plants versus WT, $^{**}P < 0.01$; *OsPHR2*-overexpressing plants versus other overexpressing plants, $^{++}P < 0.01$; Student's t-test).

C, Biomass of *PHR1-3*-overexpressing lines under hydroponic culture conditions. The 30-d-old seeding biomass of wild type (WT), *OsPHR1-Ov1*, *OsPHR2-Ov1*, *OsPHR3-Ov1* and *OsPHR3-Ov8* were measured under Pi-sufficient and Pi-deficient conditions. Values represent means ± SD of ten replicates. Data significantly different from corresponding controls are indicated ($^{**}p < 0.01$; Student's *t*-test).

plants. DNA gel blot and qRT-PCR analysis confirmed that independent *OsPHR3*-overexpressing lines (*OsPHR3*-Ov) were produced (**Figure S4**). Two single-copy *OsPHR3-Ov* lines (*PHR3-Ov1* and *PHR3-Ov8*), together with *OsPHR1*- and

158 *OsPHR2*-overexpressing plants (*PHR1-Ov1* and *PHR2-Ov1*) (**Zhou et al., 2008**), were used for
159 further analysis. The accumulation of Pi in shoots was significantly increased in *PHR3-Ov*
160 compared with WT, while Pi levels in *PHR3-Ov* were slightly higher than in *PHR1-Ov1* but
161 lower than that in *PHR2-Ov-1* plants under Pi-sufficient conditions (**Figure 2**). In accordance
162 with previous results (**Zhou et al., 2008**), no significant difference in root Pi concentrations were
163 observed between wild-type plants and overexpressors (**Figure 2B**). We also notice that the
164 shoot biomass of *OsPHR3-Ov* was higher than WT under Pi-deficient conditions, while
165 *PHR2-Ov* was lower both on Pi-sufficient and Pi-deficient conditions (**Figure 2C**), indicating a
166 character for OsPHR3 in tolerance to low Pi stress.

167 A typical trait stimulated by Pi starvation is the elongation of root hairs, which occurs in
168 both rice and Arabidopsis (**Wissuwa, 2003; Yi et al., 2005**). To determine whether all three PHR
169 proteins play roles in determining root hair morphology, we examined the root hairs of the
170 corresponding mutants and overexpression lines grown under both Pi-free and Pi-replete
171 conditions. Root hair elongation was slightly inhibited in the single mutants *phr1*, *phr2*, *phr3* and
172 the double mutants *phr1/2*, *phr1/3* and *phr2/3* (**Figure 3A and 3C**). However, root hair growth
173 was seriously repressed in the triple mutant *phr1/2/3* (**Figure 3A and 3C**). These results are
174 consistent with the results observed in Arabidopsis (**Busto et al., 2010**). Under Pi-replete
175 conditions, the root hairs were longer in overexpression lines than in the wild type (**Figure 3B**
176 **and 3D**). In accordance with the root hair elongation of *OsPHR2-Ov-1* (**Zhou et al., 2008**), the
177 *OsPHR1*-and *OsPHR3*-overexpressing lines also exhibited increased root hair elongation under
178 Pi-replete conditions, while this response was weaker than that of the *OsPHR2* overexpressor.

179 Taken together, the physiological and morphological of *phr* mutants and their overexpression
180 lines indicate that PHR1-PHR3 are functional redundancy in regulating Pi starvation response
181 and Pi-homeostasis in rice.

182 **Molecular analysis reveal partial functional redundancy as well as functional diversity**
183 **among PHR1-PHR3**

184 Now that PHR1-PHR3 show functional redundancy based on physiological and morphological
185 analysis, we examined the effects of *phr1*, *phr2* and *phr3* mutants on the Pi-starvation response
186 by examining the expression of Pi-starvation responsive (PSI) genes downstream of *OsPHR2*,
187 including *OsIPS1* (**Zhou et al., 2008**), *OsPT2* (**Liu et.al., 2010**) and *OsmiR827* (**Wang et. al.,**

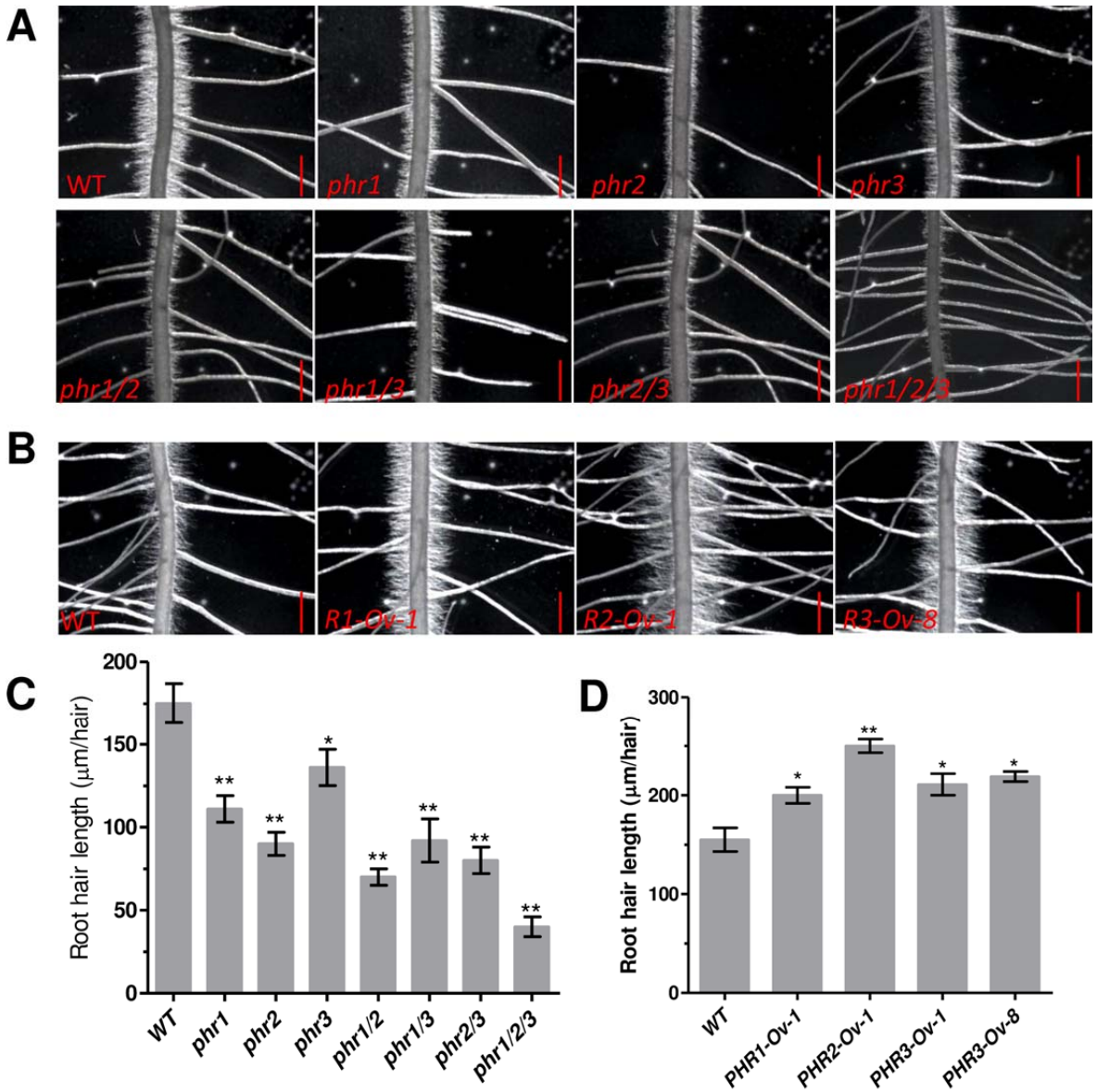

Figure 3 Effect of *PHR1-3* on root hair growth

A, Primary root hairs of 8-d-old *phr1*, *phr2*, *phr3*, *phr1/2*, *phr1/3*, *phr2/3* and *phr1/2/3* mutants were observed under Pi-free conditions (0 μM Pi). B, Primary root hairs of 8-d-old *PHR1-3*-overexpressing lines under Pi-sufficient conditions (200 μM Pi). Bars = 2 mm. C and D, The root hair length mearurement of related mutants and over expression lines. The area from 1 to 1.5 cm under the seeds were measured. Data are means ± SD (n=6). Asterisks indicate significant differences from WT (*$P < 0.05$, ** $P < 0.01$ Student's t-test).

2012). Although these mutations did not cause obvious changes in the expression of PSI genes in plants grown under a high-Pi (200 μM Pi) regimen compared with wild type, the expression of most of these genes was significantly reduced in plants cultured in solution lacking Pi (**Figure**

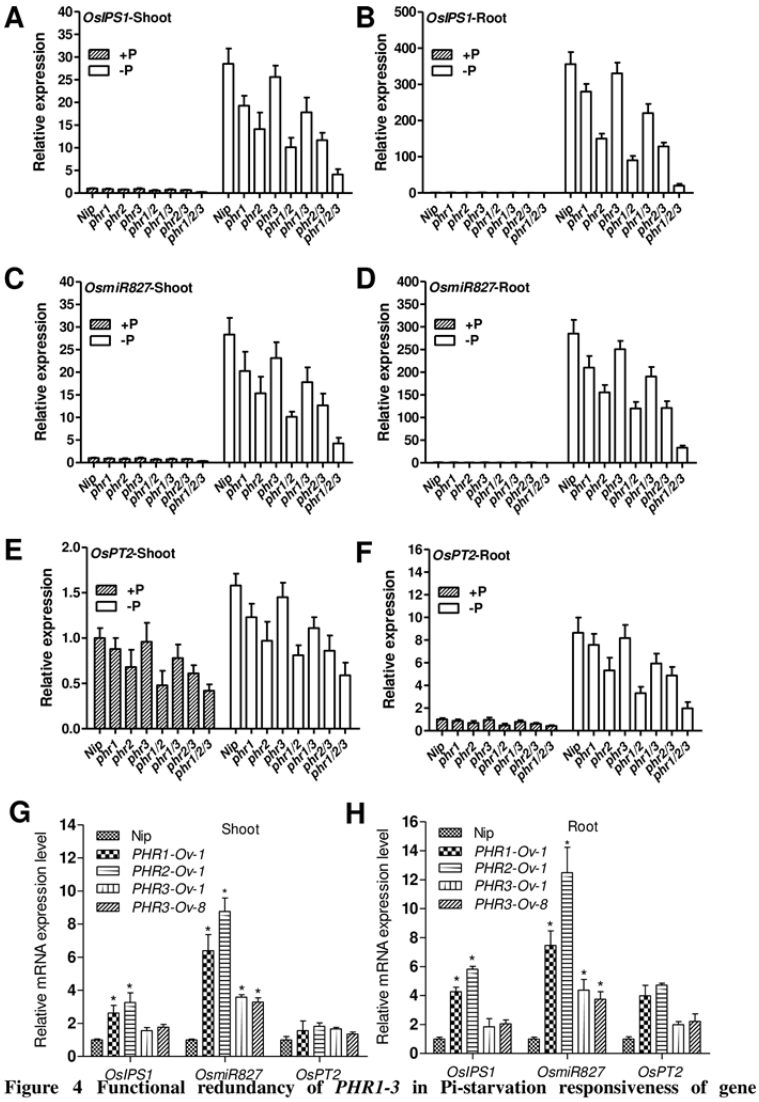

Figure 4 Functional redundancy of *PHR1-3* in Pi-starvation responsiveness of gene expression

qRT-PCR analysis of the effect of *phr1*, *phr2* and *phr3* mutants, *phr1/2, phr1/3* and *phr2/3* double mutants, and *phr1/2/3* triple mutant on the expression of Pi starvation-responsive marker genes. Two-week-old plants grown in Pi-sufficient (200 μM Pi) solution were transferred to Pi-sufficient or P-lacking solution for 7 d; RNA from roots and shoots was isolated separately and qRT-PCR was performed using specific primers (**See Table S1**) for *OsIPS1* (A and B), *OsmiR827* (C and D), *OsPT2* (E and F). The expression of wild type under Pi-sufficient condition was set to 1. Values represent means ± standard deviation (SD) of three replicates.

G and H, qRT-PCR analysis of the expression of Pi starvation-responsive genes in the *PHR1-3*-overepressing plants. RNA from roots and shoots was isolated separately from 20-d-old plants grown in Pi-sufficient (200 μM Pi) solution, and qRT-PCR was performed using specific primers (**See Table S1**) for *OsIPS1, OsmiR827* and *OsPT2*. Asterisks indicate significant differences from WT ($P < 0.05$, Student's t-test).

4A-4F). The reduced expression of *OsIPS1*, *OsPT2* and *OsmiR827* under Pi-starvation conditions was less pronounced in *phr3* than *phr1* and *phr2* (**Figure 4A-4F**). We observed synergistic and additive effects of *phr1*, *phr2* and *phr3* on the expression of all PSI genes

examined. Besides, overexpression of *OsPHR3*, like as *OsPHR1* and *OsPHR2*, can induce Pi starvation response (**Figure 4G-4H**). As the results shown, significant but lower upregulation of the examined PSI genes was observed in *PHR1-Ov1* and *PHR3-Ov1/8* plants compared with *PHR2-Ov1* plants (**Figure 4G-4H**).

To further understand the functional redundancy and diversity of PHRs, we carried out comparative microarray analysis of WT, *phr1*, *phr3* and *phr1/2/3*. The results showed that 78 transcripts were induced in the *phr1* mutant compared to WT (among these were 26 Pi-starvation induced transcripts and 8 Pi-starvation repressed transcripts). In addition, 158 genes were repressed in the *phr1* mutant compared to WT (including 77 and 12 that were induced and repressed, respectively, by Pi starvation). In the *phr3* mutant, 169 transcripts (including 48 Pi-starvation induced and 25 Pi-starvation repressed) were induced and 155 transcripts (including 51 were Pi-starvation induced and 10 were Pi-starvation repressed) were repressed compared to WT. There were 2115 transcripts (including 1072 Pi-starvation induced and 99 Pi-starvation repressed) induced and 2224 transcripts (641 were Pi-starvation induced and 74 were Pi-starvation repressed) repressed in the triple mutant *phr1/2/3* compared to WT (**Figure 5**). Some transcripts (33 induced and 32 repressed) displayed a similar pattern in both *phr1* and *phr3* mutants, but most were different, indicating that OsPHR1 and OsPHR3 function differently in some processes. Thus, these results demonstrate that PHR1-PHR3 have functional redundancy and divergence in function as well.

Different expression patterns of PHR1-PHR3 in time and space

Since PHR1-PHR3 are functional diversity in regulating Pi-starvation response and plant growth based on above mentioned results, it promote us to investigate their specific expression pattern. Firstly, mRNA expression level of *PHR1-PHR3* at different growth stages was analyzed by qRT-PCR (**Figure S5**). *PHR1-PHR3* were expressed throughout all stages of plant growth, indicating the importance of these three PHR proteins for the growth of rice. No marked changes in the expression levels of *OsPHR1* or *OsPHR2* were observed in leaves between days 10 and 70. However, the expression of *OsPHR3* increased dramatically in leaves before the booting stage (approximately day 50). This result is typical of the difference in expression between *OsPHR3* and *OsPHR1/2*.

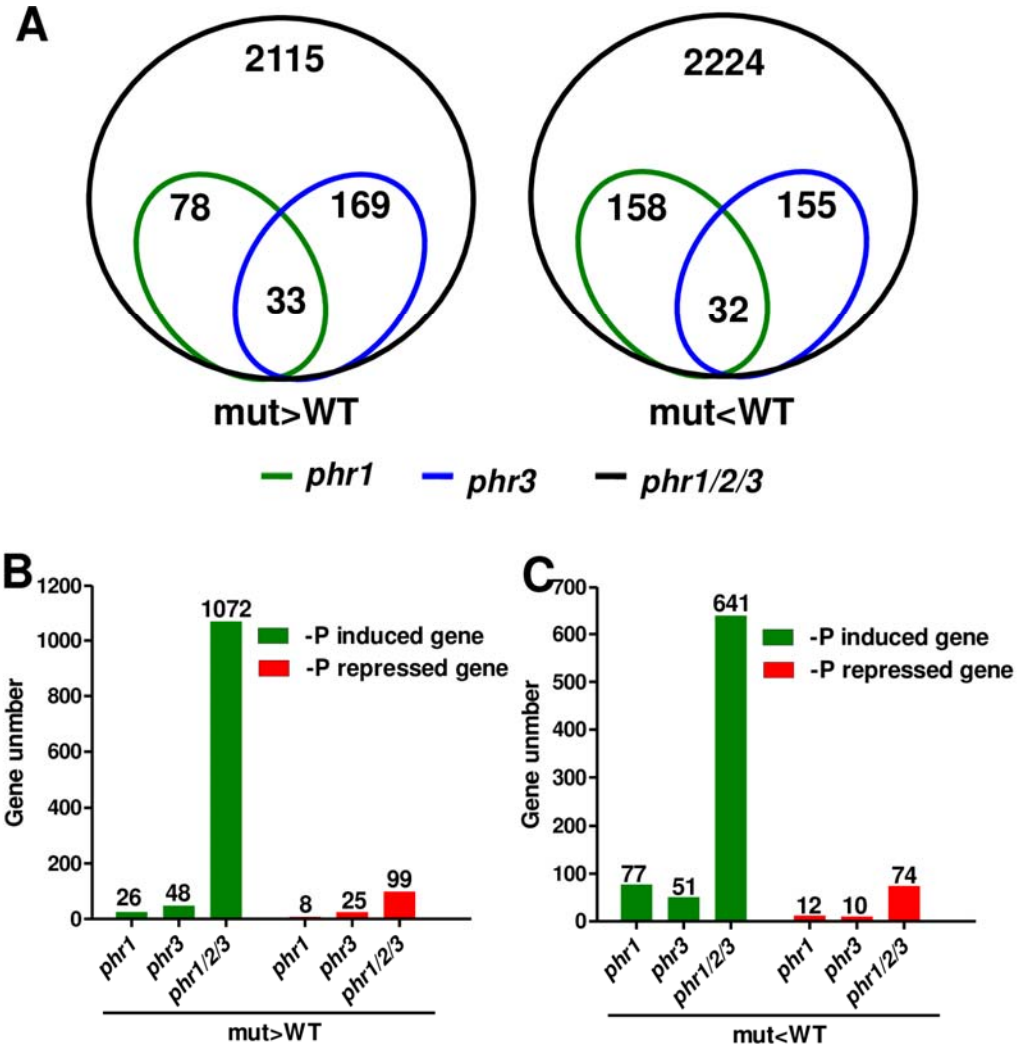

Figure 5 Comparative transcriptomes of *phr* mutants

A, Venn diagrams depicting the genes with altered expression in *phr* mutants compared to WT. The total shoot RNA of WT, *phr1*, *phr3*, and *phr1/2/3* seedlings transferred for 7 d to –Pi conditions was isolated for microarray analysis. Three repeat microarrays were performed for each material. The number of transcripts whose expression was higher [mutation (mut) > WT] or lower (mut < WT) in *phr1*, *phr3*, and *phr1/2/3* plants than in WT plants is shown.

B and C, The number Pi-starvation induced (green bar) or repressed (red bar) genes with altered expression in *phr1*, *phr3* and *phr1/2/3* mutants.

Next, to investigate the tissue-specific expression patterns of the three *PHR* genes in detail, we generated plants harboring P_{PHR1}*:GUS*, P_{PHR2}*:GUS* and P_{PHR3}*:GUS*. Examination of tissue cross-sections indicated that *OsPHR1*, *OsPHR2* and *OsPHR3* were all expressed in the root cap

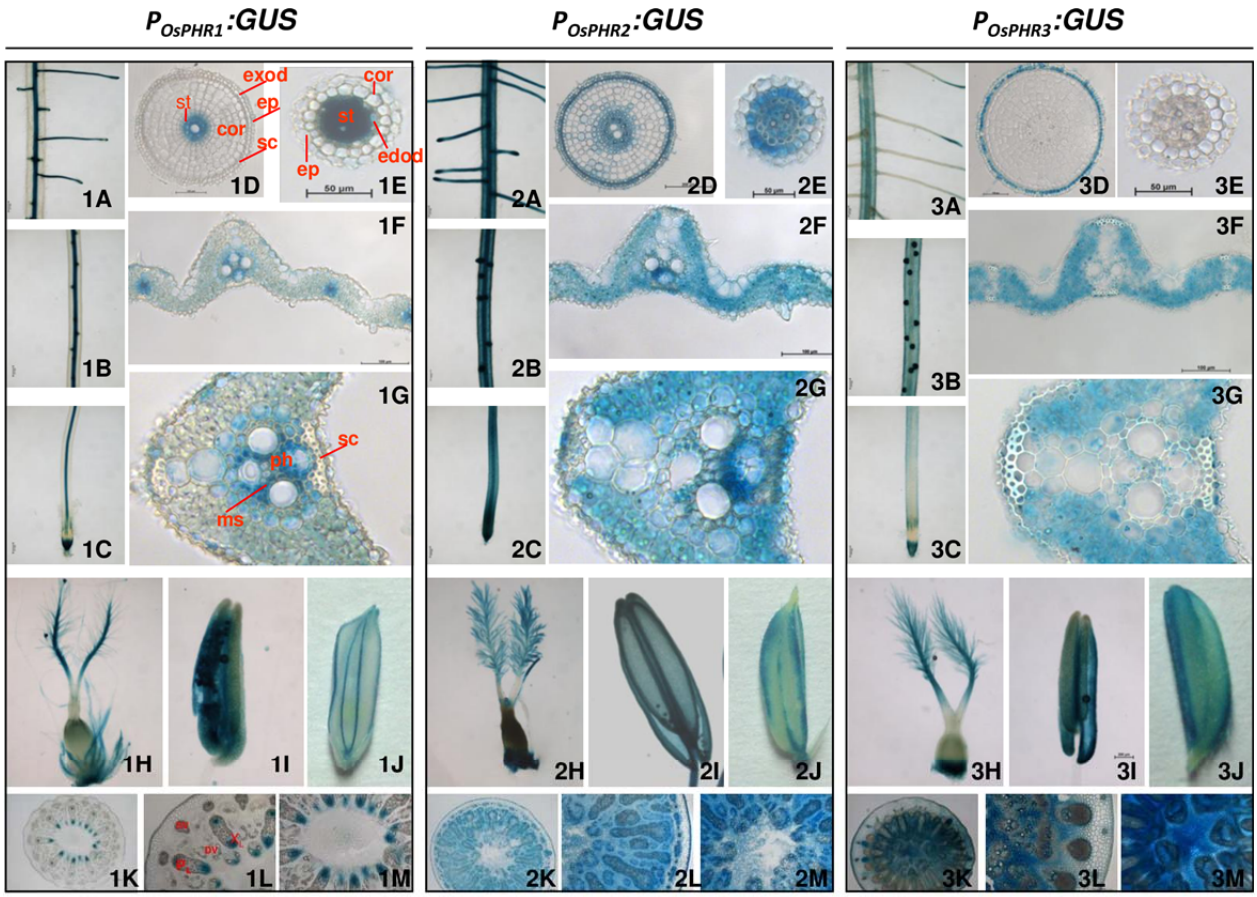

Figure 6 Tissue-specific expression patterns of *OsPHR1, OsPHR2* and *OsPHR3*

Tissue-specific expression patterns of *OsPHR1, OsPHR2* and *OsPHR3* indicated by expression *POsPHR1:GUS* (images 1A-1M), *POsPHR2:GUS* (images 2A-2M) and *POsPHR3:GUS* (images 3A-3M) fusions in the transgenic plants. In each panel (1-3), images A-C show GUS staining of the primary root: root cap, meristematic zone and elongation zone (C), maturation zone (B,C); Bars in 1-3 = 0.5 mm. (4-5) Cross sections of root elongation zone (D), lateral root (E); Bars = 50 μM. Cross section of GUS-stained leaf blade (F, G); Bars = 100 μm. (H-J) GUS staining of pistil, stamens and shell; (K-M) Cross section at the center of node I. **ms**: mestome sheath cell, **xm**: xylem; **ph**: phloem; **sc**: sclerenchyma cell; **exod,** exodermis; **ep**: epidermis; **cor,** cortex, **st**, stele; **XL**: Xylem region of large vascular bundles; **PL**: phloem region of large vascular bundles; **SV**: small vascular bundle; **DV**: diffuse vascular bundle.

(**Figure 6 1C, 2C, 3C**), while in the remaining part of the primary root, *OsPHR1* was expressed in the vascular tissues (**Figure6 1D**), *OsPHR2* was expressed in the exodermis, sclerenchyma and vascular tissues (**Figure 5 2D**), and *OsPHR3* was expressed only in the exodermis (**Figure 6 3D**). In the lateral root, *OsPHR1* was expressed in the stele (**Figure 6 1E**) and *OsPHR2* was

expressed in the cortex cells and stele cells (**Figure 6 2E**), but no signal was detected in the lateral roots of *OsPHR3* except at the root tip (**Figure 6 3E**). GUS staining of *OsPHR2* and *OsPHR3* was also detected in all mesophyll cells of the leaf (**Figure 6 2F, 2G, 3F, 3G**), while *OsPHR1* was expressed only in the mestome sheath cells and the phloem cells of the leaf (**Figure 6 1F, 1G**). In flowers, GUS staining of *OsPHR1*, *OsPHR2* and *OsPHR3* were observed in pollen, the vascular cylinder of the anther and the veins of the lemma, palea and pistils (**Figure 6 1H-1J, 2H-2J, 3H-3J**). In node I, *OsPHR1* was localized to the xylem and phloem region of large vascular bundles (X_L and P_L) (**Figure 6 1K-1M**) and *OsPHR3* was localized to the xylem and phloem region of large vascular bundles, small vascular bundles (SV), and diffuse vascular bundles (DV) (**Figure 6 3K-3M**), while *OsPHR2* was expressed in all node I tissues (**Figure 6 2K-2M**). These expression pattern differences also hint that PHR1-PHR3 are functional diversity in regulating crop growth.

Different DNA binding affinity of PHR1-PHR3

Given the partial functional redundancy among OsPHR1, OsPHR2 and OsPHR3 and their differential effects on the expression of various PSI genes (as shown by our analysis of *phr1, phr2* and *phr3* single, double, triple mutants and overexpressors), we next examined whether these proteins have similar DNA binding properties by performing yeast one-hybrid assays (Y1H) and electrophoretic mobility shift assays (EMSAs). The *cis*-element PHR1-binding sequence (P1BS; GNATATNC) contains two variant bases. In order to understand the differences in DNA binding affinities between the three PHR proteins, we tested PHR proteins with different combinations of the two variant bases in the P1BS by Y1H assay. The P1BS binding affinity of OsPHR2 was the highest among the proteins, while that of OsPHR3 was the lowest (**Figure 7A and 7B**). When the first variant base of the P1BS was changed to "T", "C" or "G", the DNA binding affinities for all three PHR proteins were significantly decreased compared with original P1BS (GaATATcC). When the second variant base was substituted by "A" or "G", there was no obviously change in binding affinity. By contrast, when the second variant base was substituted by "T", the DNA binding affinities significantly increased for all three PHR proteins. We also observed that the P1BS variant "GaATATtC" was the most efficient for PHR1-3 binding, and so we named it the high affinity P1BS (HA-P1BS). Conversely, the P1BS form "GgATATgC" was the lowest affinity P1BS for PHR1-PHR3, and we named it the low affinity P1BS (LA-P1BS). To further understand the DNA binding affinity

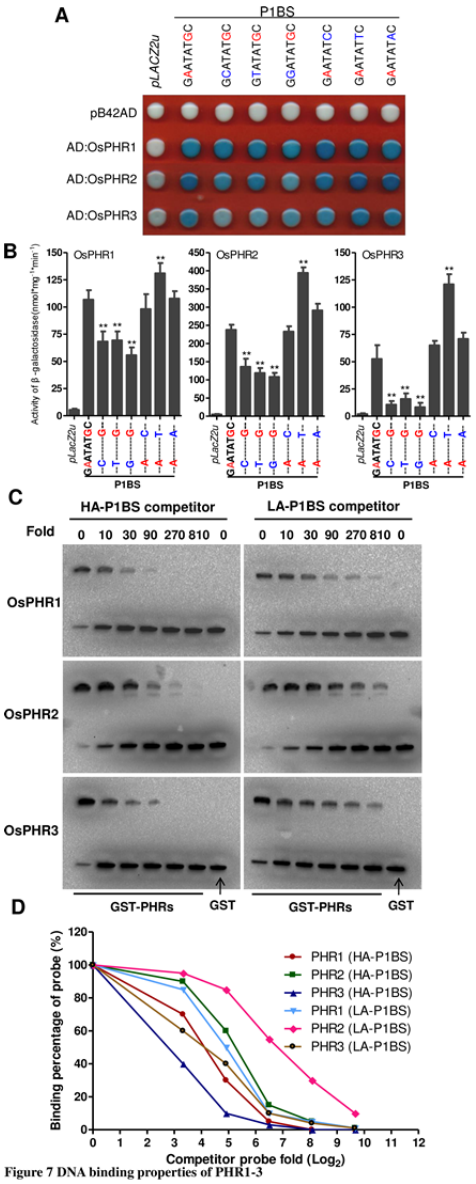

Figure 7 DNA binding properties of PHR1-3

A, Yeast one-hybrid assays of the DNA binding affinity of PHR1-3 for different P1BS types. The variant bases in the P1BS motif of *OsIPS2* were substituted by different bases as indicated; pLacZ2u was used as a negative control.

B, *β*-galactosidase of activity measurement of PHR1-3 binding to different P1BS versions. Values represent means ± SD of five replicates. Data significantly different from corresponding controls are indicated (Original P1BS versus the substituted P1BS, $^{**}P < 0.01$, Student's t-test).

C, EMSA showing that PHR1-3 preferentially bind to the P1BS GaATATtC (High affinity P1BS, HA-P1BS) rather than GgATATgC (Low affinity P1BS, LA-P1BS). The binding between GST-PHR1-3 and biotin-labeled LA-P1BS was competed by different amounts of unlabeled competitor (HA-P1BS or LA-P1BS). GST protein was used as negative control. The protein amount used was 50 ng per lane, the biotin-labeled DNA probe was 20 fmol per lane. The fold excess of the competitor relative to the labeled probe is indicated above the lane.

D, Relative binding percentage of PHR1-3 competed by increasing amounts of unlabeled HA-P1BS or LA-P1BS, quantified from experiments shown in C. The first lane without competitor was set as 100%.

differences of PHR1-3, DNA binding affinity competition experiments were performed using EMSA. PHR1-PHR3 were individually allowed to bind biotin-labeled LA-P1BS probe, then different amounts of unlabeled P1BS (HA-P1BS or LA-P1BS) were added. With increasing

amounts of competitor, the percentage of bound probe decreased. OsPHR3 showed the most rapid decline in binding while OsPHR2 binding decreased most slowly, indicating OsPHR3 has the lowest binding affinity and OsPHR2 the highest (**Figure 7C and 7D**). As predicted, HA-P1BS was more efficient than LA-P1BS at competing with the bound probe. Together, these results demonstrate that all three PHR proteins bind to the P1BS motif, with different binding affinities for different types of P1BS.

OsPHR3 displays improved growth performance in low Pi soils

Overexpression of *OsPHR2* reduces plant growth under both normal and Pi-deficient conditions (**Zhou et al., 2008**). Similarly, overexpression of *OsPHR1* did not confer tolerance to low Pi stress, although it did not cause significant growth retardation under normal conditions. By contrast, *OsPHR3* overexpressing lines did not exhibit reduced plant growth under Pi-sufficient conditions, and they exhibited enhanced growth under Pi-deficient hydroponic conditions compared with the wild type (based on biomass measurements; **Figure 2C**). To rule out the possibility that the higher protein expression levels in *OsPHR2-Ov* lines resulted in the retarded growth, *OsPHR2* and *OsPHR3* tagged overexpression lines were also analyzed (**Figure S6C**). The results showed that even when the OsPHR2 protein level was lower than that of OsPHR3, the *OsPHR2* overexpressor still showed growth inhibition (**Figure S6 A, B and D**). These results suggested that *OsPHR3-Ov* could be utilized in agricultural production systems to enhance crop tolerance of low-Pi conditions.

In a further step, we examined the growth of *OsPHR3-Ov* in pots. The grain yield, total P concentration and effective panicle number were higher in *OsPHR3-Ov* lines than in the wild type (**Figure 8**), implying that *OsPHR3-Ov* lines tolerate low Pi conditions, which is in accordance with our hypothesis. To further confirm that overexpression of *OsPHR3* is beneficial to crop growth under Pi-deficient conditions, we performed field experiments. The results show that the biomass, production and total P in shoots and grains were higher in the *OsPHR3-Ov* lines than in the wild type under three Pi gradient levels (**Figure S7**). Furthermore, the production of grain products of *OsPHR3-Ov* lines under moderate Pi fertilizer (MP) conditions was almost equal to that of the wild type under Pi-sufficient (HP) conditions. Taken together, these results suggest that *OsPHR3* would be a useful candidate gene for breeding crops tolerant to low-Pi stress.

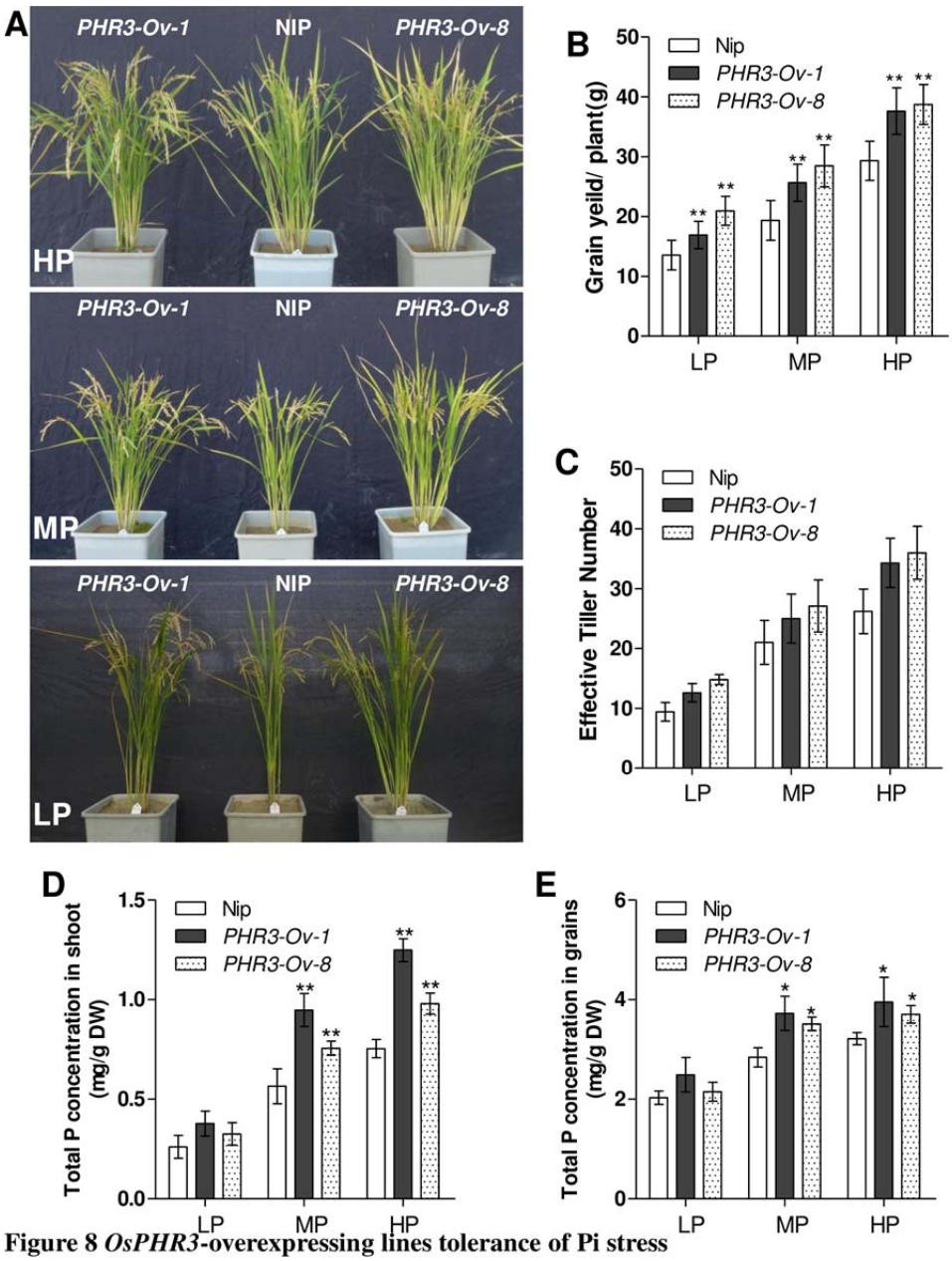

Figure 8 *OsPHR3*-overexpressing lines tolerance of Pi stress

A, Growth performance of the wild-type (Nip) and transgenic plants *OsPHR3-Ov-1/8* grown in pots with high-Pi fertilizer (200 mg/kg Pi, HP), moderate-Pi fertilizer (100 mg/kg Pi, MP) and low-Pi fertilizer (30 mg/kg Pi, LP). B and C, the grain yields and numbers of effective panicles per plant; data are means ± SD (n=4); D and E, Total P concentration in shoot and grains; data are means ± SD (n=4). Data significantly different from corresponding controls are indicated (*p < 0.05; **p < 0.01 Student's t-test).

294

Discussion

The response of higher plants to Pi starvation is a complicated process in which numerous genes are activated or repressed at the transcriptional or post-transcriptional level, leading to changes in physiological and morphological processes (**Franco-Zorrilla et al., 2004; Yang and Finnegan, 2010**). While much research has focused on this process, information about the OsPHR TF network in rice is currently limited. In this study, we characterized the roles of three OsPHR proteins in regulating Pi signaling and homeostasis in rice. Functional redundancy was confirmed based on the results of physiological morphological effects of *PHR1-PHR3* mutants and overexpressors, and the transcriptomic analysis of mutants. The different expression patterns and DNA binding affinities of these OsPHR proteins reflects their functional diversity in regulating the plant response to Pi starvation. Furthermore, the results of this study highlight the potential utility of *OsPHR3* for molecular breeding in agriculture systems.

Function redundancy of PHR1-PHR3

The regulatory mechanisms of PHR1 proteins in Arabidopsis and rice are similar (**for review, Chiou et al., 2011; Wu et al., 2013**). Nonetheless, there are some differences in the functions of PHR1 family members. AtPHR1 and OsPHR2 are central regulators in Arabidopsis and rice, respectively (**Bustos et al., 2010; Wu et al., 2013**). Like the *phr1* mutant in Arabidopsis (**Rubio et al., 2001**), the *phr2* mutant in rice exhibited dramatically inhibited Pi starvation signaling (**Figure 4A-4F**). Although mutations in the two other *OsPHR* genes also disrupted Pi starvation signaling, the degree of reduction was weaker compared with that of the *phr2* mutant. Furthermore, examination of the double and triple OsPHR mutants revealed that *OsPHR1*, *OsPHR2* and *OsPHR3* are functionally redundant in regulating Pi starvation signaling, which is similar to the roles of *AtPHR1* and *AtPHL1* in Arabidopsis (**Bustos et al., 2010**). However, there are some differences in Pi homeostasis between AtPHRs and OsPHRs. For example, the *phr1*, *phl1* and *phr1/phl1* mutants in Arabidopsis exhibit disrupted Pi homeostasis, leading to reduced Pi levels in the plant, but this was not observed in *phr1*, *phr2* or *phr3* in rice. Pi homeostasis was affected only when three *OsPHR* genes were mutated (**Figure 1C**). In Arabidopsis, two highly important Pi transporter genes, *AtPht1;1* and *AtPht1;4* (**Shin et al., 2004**), as well as *TRANSPORTER TRAFFIC FACILITATOR 1* (*AtPHF1*) (**González et al., 2005; Bayle et al., 2011**), are directly regulated by AtPHRs, which may explain why *AtPHR* mutants exhibit

reduced Pi levels. Of the 13 Pi transporter genes in the rice genome **(Paszkowski et al., 2002; Goff et al., 2002**), *OsPT8* is one of the most important, since half of the Pi uptake capacity depends on the presence of OsPT8, a high-affinity Pi transporter (**Chen et al., 2011; Jia et al., 2011**). In addition, OsPHF1 plays a key role in regulating the plasma membrane localization of Pi transporters. Mutation of *OsPHF1* also severely reduces Pi accumulation (**Chen et al., 2011**). However, *OsPHF1* is not directly regulated by OsPHR2 in rice (**Chen et al., 2011**). The current results also show that there was little reduction in the expression of *OsPHF1* and *OsPT8*, even in the triple mutant *phr1/2/3* (**Figure S8**), perhaps because mutation of rice *PHRs* does not obviously affect Pi-homeostasis as it does in Arabidopsis. We also noticed that the growth of triple mutant *phr1/2/3* was greatly inhibited under both Pi-sufficient and Pi-deficient conditions (**Figure 1A and 1B**), although there was little reduction in Pi levels in the triple *phr1/2/3* mutant. These results suggest that other unknown factors in addition to Pi levels affect the growth of *phr1/2/3*. Indeed, OsPHRs mediate other regulatory pathways that are essential for the normal growth of rice, such as light, iron and oxygen signaling pathways (**Nilsson et al., 2012; Bournier et al., 2013; Klecker et al., 2014**).

PHR1/PHL1 play a key role in regulating the root-to-shoot ratio, since this ratio is higher in the Arabidopsis *phr1/phl1* mutant than in the wild type (**Bustos et al., 2010**). However, this ratio was not obviously altered in rice mutants *phr1*, *phr2*, *phr3*, *phr1/2*, *phr1/3*, *phr2/3* and *phr1/2/3* (**Figure S9**). Although the triple mutant *phr1/2/3* exhibited greatly reduced growth, no obvious changes in this ratio were observed compared to wild type (**Figure S9**), since both shoot and root growth were inhibited in *phr1/2/3*.

PHR1-3 show functional diversity

In general, more than one functionally similar TF family member plays the same role in responses to a given abiotic or biotic stress. For example, bHLH transcription factors MYC2, MYC3 and MYC4 function in regulating jasmonate (JA) responses (Boter et al., 2004; Lorenzo et al., 2004; Dombrecht et al., 2007; Ferna´ndez-Calvo et al., 2011). Similarly, a group of PHR TFs have similar functions in regulating the Pi starvation response by binding to the P1BS motif to regulate downstream genes that function in these responses (Rubio et al., 2001; Zhou et al., 2008; Bustos et al., 2010; Liu et al., 2011; Wang et al., 2014). While all three OsPHRs take part in the same Pi regulatory pathway, there are clear differences between. *OsPHR1* is expressed

mainly in the vascular bundle, suggesting that it plays a role in regulating Pi translocation from roots to shoots and in Pi signal transduction (**Figure 6**).

In addition, *OsPHR3* and *OsPHR1/2* exhibit the differences in their mRNA expression levels in response to Pi-deficient conditions; *OsPHR3* was induced under Pi starvation conditions, while *OsPHR1* and *OsPHR2* were not (**Figure S10**). These results indicate that *OsPHR1* and *OsPHR2* are transcribed throughout normal plant growth, while *OsPHR3* is only transcribed when plants are faced with Pi deficiency, perhaps explaining why *OsPHR3* was induced at the flowering stage, during which more energy and Pi are needed for flower production (**Figure S5**). Indeed, *Brassica napus PHR1* (*BnPHR1*) and *Triticum aestivum* PHR1 (*TaPHR1*) are induced under Pi-deficient conditions, while *AtPHR1* and *AtPHL1* are not (**Rubio et al., 2001; Zhou et al., 2008; Bustos et al., 2010; Ren et al., 2012; Wang et al., 2013**). We also noticed that all the three *OsPHRs* were expressed in the root tip (**Figure 6**), which is the most important tissue for Pi sensing and uptake from the environment (**Zhang et al., 2014**), implying their co-regulation in this tissue. Moreover, much of the genes regulated by OsPHR1 and OsPHR3 are different based on the microarray analysis (**Figure 5**), indicating that OsPHR1 and OsPHR3 mediate in different regulation process in rice.

TF binding sites and flanking sequences can affect TF DNA binding affinity (**Rajkumar et al., 2013**). In this study, OsPHR proteins exhibited different P1BS binding affinities (**Figure 7**) and their binding abilities were affected by variant bases in P1BS as Ruan et al reported (**Ruan et al., 2015**). How the P1BS variant bases influence these affinities will be a subject of further study.

Overexpression of OsPHR3 confers tolerance to low-Pi stress in rice

Overexpression of *AtPHR1*, *OsPHR2* and *BnPHR1* leads to Pi accumulation in shoots, producing a necrotic phenotype in leaves and growth repression under normal conditions (**Rubio et al., 2001; Zhou et al., 2008; Bustos et al., 2010; Ren et al., 2012**). By contrast, overexpression of *TaPHR1* promotes the growth of wheat under Pi-deficient conditions (**Wang et al., 2013**). These studies demonstrate that there are species-specific differences in PHR TFs. In the current study, three *PHR*-overexpressing lines exhibited different phenotypes in the face of various Pi levels (**Figure 2A, Figure 8A and Figure S6A-B**). *OsPHR2* overexpressors exhibited

retarded plant growth, while *OsPHR3-Ov* lines exhibited low-Pi stress tolerance under hydroponic, pot, and field conditions (**Figure 4A, Figure 8A, Figure S6A-B**). Perhaps the better growth of the *OsPHR3-Ov* lines is due to the low DNA-binding affinity of OsPHR3 compared with OsPHR2. Some genes that play positive roles in abiotic stress (such as Pi deficiency) resistance pathways may have negative effects on growth and development; OsPHR3 might bind less effectively to such genes than OsPHR2. Considering the different binding affinities of OsPHRs with different types of P1BS, this explanation appears to be reasonable, and it may account for the observation that overexpression of *OsPHR2* inhibited plant growth, even under low-Pi conditions, in which the Pi content was below toxic levels that repress plant growth (**Zhou et al., 2008**). These findings imply that not only the Pi levels affect the growth of *OsPHR2-Ov* plants, but also other factors triggered by OsPHR2 also affect plant growth under normal conditions. Furthermore, transcriptomic analysis of of *phr* mutants showed that the expression level of some auxin responsive, photo-system and redox-system related genes were induced or repressed, indicating PHRs is an sophisticated regulation system in regulating plant growth.

In summary, we compared and analyzed the integrated regulatory effects of three OsPHR proteins on Pi signaling and Pi homeostasis in rice. Our findings provide evidence that their functional redundancy and diversity enable them to co-regulate the Pi response of rice.

Method and materials

Plant materials and growth conditions

The *phr1* mutant (*Oryza sativa* ssp. *japonica* cv. Nipponbare) was obtained via the Crisper/Cas technique (**Feng Z, et al., 2013**), and the recognition site (5'-GATTCTGTGTCTAGC CATGA-3') was designed at the first exon. The mutation site of *phr1* was identified by sequencing analysis (**Figure S2**). The primers used for identification of *phr1* are listed in **Table S1**. The *phr3* T-DNA insertional mutant (NE3009) (ssp. *japonica* cv. Nipponbare) was obtained from CIRAD (Centre de Coopération International en Recherche Agronomique pour le Développement; http://orygenesdb.cirad.fr). The *phr3* T-DNA insertion site at the seventh exon was characterized by sequencing analysis (**Figure S3**). The primers used to identify the *phr3* mutant are listed in **Table S1**. The identification of the *phr2* T-DNA insertional mutant was performed as described (**Chen et al., 2011**). The *phr2* mutant was backcrossed for three generations with Nipponbare (NIP) prior to analysis. The primers are listed in **Table S1.**

To generate a double mutant containing mutations or insertions in *OsPHR1* and *OsPHR2*, a *phr1* homozygous allele was crossed with a *phr2* homozygous allele. Double mutants were obtained from the F1 population, which were designated *phr1/2*. The other double mutants, designated *phr1/3* and *phr2/3*, were obtained using the same method, as was the triple mutant, designated *phr1/2/3*. The primers used to identify the mutations are listed in **Table S1.**

The hydroponic experiments were performed using rice solution culture (**Zhou et al., 2008**). Rice plants were grown in a greenhouse with a 12/12 light/dark cycle (200 $molm^{-2}$ s^{-1} photon density) at 30/22°C after germination. Humidity was maintained at approximately 60%. The soil pot experiments were performed as described previously (**Zhou et al., 2008**).

RNA extraction, RT-PCR and quantitative PCR assay

RNA was isolated from roots and shoots using Trizol reagent (Invitrogen) followed the manufacturer's instructions. Reverse transcription was performed using a Moloney Murine Leukemia Virus Reverse Transcriptase (M-MLV RT) cDNA synthesis kit (Promega) according to the manufacturer's instructions. Quantitative real-time qRT-PCR was performed as previously described (Zhou et al., 2008), briefly the wild type expression was normalization to 1. Detection

and quantification of mature *miR399* and *miR827* were performed as previously described (Varkonyi-Gasic et al., 2007). The primers used for qRT-PCR analysis are listed in **Table S1.**

Construction of vectors and plant transformation

The *OsPHR3* overexpression vector was constructed as follows. Full-length *OsPHR3* was cloned and inserted into the *pFLAG122* vector after digestion with *Kpn*I and *Xba*I. The primers are listed in **Table S1.**

To produce transgenic plants expressing the *GUS* reporter gene, P_{OsPHR1}-*GUS*, P_{OsPHR2}-*GUS* and P_{OsPHR3}-*GUS*, the Nipponbare genomic DNA fragments containing promoter regions less than 3 kb in size (from start codon ATG) were amplified with the primer pairs OsPHR1-P-GUS-F (BamHI)/OsPHR1-P-GUS-R (KpnI), OsPHR2-P-GUS-F (SalI)/OsPHR2-P-GUS-R (BamHI) and OsPHR3-P-GUS-F (BamHI)/OsPHR3-P-GUS-R (KpnI) and cloned into the modified *pCAMBIA1300-GUS* plasmid (**Lv et al., 2014**), respectively. The primers are listed in **Table S1.**

The CRISPR (clusters of regularly interspaced short palindromic repeats)/Cas9 endonuclease system is a site-specific genomic editing tool used in many organisms (**Hale et al., 2009; Jore et al., 2011; Carroll, 2012; Jinek et al., 2012**), including plants (**Feng et al.; 2014**). The *OsPHR1* CRISPR vector was constructed following previously published protocols (**Feng et al., 2013**) using the primers listed in **Table S1**. The constructed vectors were transformed into rice (Nipponbare) via *Agrobacterium tumefaciens* EHA105-mediated transformation as described previously (Chen et al., 2003).

GUS histochemical analysis

The T_1 seeds of P_{OsPHR1}:*GUS*, P_{OsPHR2}:*GUS* and P_{OsPHR3}:*GUS* transgenic plants were grown in standard rice culture solution. The roots and shoots of 10-d-old seedlings, stamens, pistils, shells and nodes were subjected to histochemical GUS analysis as described (**Jefferson et al., 1987**). After staining, the sections were washed in 70% ethanol and observed under a ZEISS microscope. The roots, shoots and nodes were embedded in 2% agar and cut into 30-μm sections using a vibrating microtome (Leica) and observed/photographed through a microscope (ZEISS).

DNA gel blotting analysis

DNA was isolated from transgenic plants using a Plant Genomic DNA Kit (TIANGEN),

and the DNA was digested with HindIII and EcoRI. DNA gel blotting was performed as previously described (Zhou et al., 2008) using *G418* as the hybridization probe.

Electrophoretic mobility shift assay (EMSA)

To express the recombinant GST:OsPHR1, GST:OsPHR2 and GST:OsPHR3 proteins in *E. coli* strain *BL21*(*DE3*) (Novagen), the full-length CDS of *OsPHR1-3* were amplified with primer pairs OsPHR1-GST-F (EcoRI)/OsPHR1-GST-R (SalI), OsPHR2-GST-F (BamHI)/OsPHR2-GST-R (SalI) and OsPHR3-GST-F (BamHI)/OsPHR3-GST-R (SmaI) and cloned into the pGEX-4T-1 vector (GE Healthcare), resulting in the GST-PHR1-3 vectors. The recombinant proteins were extracted and purified according to the manufacturer's instructions (GE Healthcare Life Science). The promoter regions containing the PIBS motifs were amplified using primer pairs OsIPS1-probe-F/OsIPS1-probe-R, OsPT2-probe-F/OsPT2-probe-R and OsmiR827-probe-F/OsmiR827-probe-R, which were used to obtain biotin-labeled probes. The primer sequences are listed in **Table S1**. The EMSA was performed using a LightShift Chemiluminescent EMSA Kit (Thermo Scientific) according to the manufacturer's instructions.

Yeast one-hybrid assay

To identify and characterize the interactions between PHR1-3 and the promoter regions of *OsIPS1* and *OsmiR827* in yeast, full-length *PHR1-3* cDNA was cloned into the pB42AD vector (Clontech), thus generating pB42AD-OsPHR1 (AD:OsPHR1), pB42AD-OsPHR2 (AD:OsPHR2) and pB42AD-OsPHR3 (AD:OsPHR3) for the yeast one-hybrid assay. The promoter regions of *OsIPS1* (from -1 to -1678) and *OsmiR827* (from -1 to -1827) were cloned into *pLAZ2u* (Clontech). Yeast strain EGY48 was transformed with AD:OsPHR1, AD:OsPHR2 and AD:OsPHR3 and grown on synthetic medium lacking urea and tryptophan (Clontech). The primers and restriction endonucleases used for yeast one-hybrid analysis are listed in **Table S1**.

β-galactosidase activity measurement was performance according to Calvenzani (**Calvenzani et al., 2012**). Briefly, transformed yeast cultures grown overnight were injected in a fresh –Trp/–Ura culture solution until the yeast grew to OD_{600}=0.4. The cells were then collected to extract total proteins, and *β*-galactosidase activity was measured after treatment with reaction buffer (Z-buffer: 60 mM NaH_2PO_4, 40 mM Na_2HPO_4 anhydrous, 10 mM KCl, 1 mM Mg_2SO_4, 50 mM *β*-mercaptoethanol), stopping buffer (1.5 M $CaCO_3$) and substrate

o-nitrophenyl-β-D-galactopyranoside (ONPG: 1.4 mg/ml). The chromogenic reaction and plate reading were carried out essentially following the MatchMaker One Hybrid System manual (Clontech).

Measurement of Pi levels, total Pi and Pi uptake rate

Measurements of Pi levels, total Pi, biomass and Pi uptake ability in transgenic plants were performed as described previously (Zhou *et al.*, 2008; Wu *et al.*, 2011).

Microarray Analysis

Fifteen-day-old plants of WT, *phr1*, *phr3* and *phr1/2/3* were treated with –P for 7 d, and shoots of plants from three biological repeats were sampled for Affymetrix microarray analysis. Microarray and data analyses were performed as described (**Bustos et al. 2010**). The raw microarray data can be accessed in the Gene Expression Omnibus database (www.ncbi.nlm.nih.gov/geo) via accession no. GSE69010. The genes were considered to be Pi-starvation induced or repressed based on previously reported RNA-seq data (Accession number SRA097415) (**Secco et al., 2013**).

Statistics

Student's two-tailed *t*-test was used for all experiments to determine the significance of differences between two groups.

Acknowledgments

This work was supported by grants from the National Basic Research and Development Program of China (grant no. 2011CB100303), National High Technology Research and Development Program of China 863 (Grant 2012AA10A302), Ministry of Agriculture of China (grant no. 2014ZX08001005) and the Ministry of Education and Bureau of Foreign Experts of China.

Accession numbers in this study

Rice Genome Initiative locus identifiers for the genes mentioned in this article are Os03g21240 (*OsPHR1*), Os07g25710 (*OsPHR2*), Os02g04640 (*OsPHR3*), Os07g09000 (*OsPHF1*), Os03g05640 (*OsPT2*), Os10g30790 (*OsPT8*) and *OsACTIN* (Os03g50890). GenBank accession numbers: AY568759 (*OsIPS1*), AK240849 (*OsIPS2*); miRNA database accession numbers: MI0010490 (*OsmiR827*).

Figure legend

Figure 1 Effect of phr1 and phr2 and phr3 mutations on Pi-homeostasis

A, Phenotypic performance of 30-d-old wild type (WT) plants, *phr1*, *phr2* and *phr3* mutants, *phr1/2*, *phr1/3* and *phr2/3* double mutants, and *phr1/2/3* triple mutant under Pi-sufficient (200 μM Pi) and Pi-deficient (10 μM Pi) hydroponic conditions. Bars = 10 cm.

B and C, Histograms of dried biomass (B) and cellular Pi concentration (C) of shoots and roots of 30-d-old wild type (WT) plants, *phr1*, *phr2* and *phr3* single mutants, *phr1/2*, *phr1/3* and *phr2/3* double mutants, and *phr1/2/3* triple mutant under Pi-sufficient (200 μM Pi) and Pi-deficient (10 μM Pi) conditions. Values represent means ± standard deviation (SD) of three replicates. Data significantly different from the corresponding controls are indicated (*phr1*, *phr2* and *phr3* mutant versus wt, $^{*}P < 0.05$; *phr1*/2, *phr1*/3, *phr2*/3 double mutants, and *phr1*/2/3 plants versus other plants, $^{**}P < 0.01$; Student's t-test).

Figure 2 Overexpression of *OsPHR3* results in shoot Pi accumulation under Pi-sufficient conditions, like as *OsPHR1* and *OsPHR2*

A, Phenotypic performance of two independent OsPHR3-overexpressing plants (*OsPHR3-Ov1* and *OsPHR3-Ov8*) compared to wild type (WT) and PHR1/2-overexpressing plants (Zhou et.al, 2008) under Pi-sufficient (200 μM Pi) and Pi-deficient (10 μM Pi) conditions. Two independent lines of OsPHR3 overexpressors were confirmed by DNA gel blot analysis (See Figure S4). Bars = 10 cm.

B, Cellular Pi levels in shoots and roots of 30-d-old WT and PHR1-3-overexpressing plants grown in hydroponic culture under Pi-sufficient and Pi-deficient conditions. Data significantly different from corresponding controls are indicated (overexpressing plants versus WT, $^{**}P < 0.01$; OsPHR2-overexpressing plants versus other overexpressing plants, $^{++}P < 0.01$; Student's t-test).

C, Biomass of PHR1-3-overexpressing lines under hydroponic culture conditions. The 30-d-old seeding biomass of wild type (WT), *OsPHR1-Ov1*, *OsPHR2-Ov1*, *OsPHR3-Ov1* and *OsPHR3-Ov8* were measured under Pi-sufficient and Pi-deficient conditions. Values represent means ± SD of ten replicates. Data significantly different from corresponding controls are indicated ($^{**}P < 0.01$; Student's t-test).

Figure 3 Effect of PHR1-3 on root hair growth

A, Primary root hairs of 8-d-old *phr1*, *phr2*, *phr3*, *phr1*/2, *phr1*/3, *phr2*/3 and *phr1*/2/3 mutants were observed under Pi-free conditions (0 μM Pi). B, Primary root hairs of 8-d-old PHR1-3-overexpressing lines under Pi-sufficient conditions (200 μM Pi). Bars = 2 mm. C and D, The root hair length mearurement of related mutants and over expression lines. The area from 1 to 1.5 cm under the seeds were measured. Data are means ± SD (n=6). Asterisks indicate significant differences from WT ($^{*}P < 0.05$, $^{**}P < 0.01$ Student's t-test).

Figure 4 Functional redundancy of PHR1-3 in Pi-starvation responsiveness of gene expression

qRT-PCR analysis of the effect of *phr1*, *phr2* and *phr3* mutants, *phr1*/2, *phr1*/3 and *phr2*/3 double mutants, and *phr1*/2/3 triple mutant on the expression of Pi starvation-responsive marker genes. Two-week-old plants grown in Pi-sufficient (200 μM Pi) solution were transferred to Pi-sufficient or P-lacking solution for 7 d; RNA from roots and shoots was isolated separately and qRT-PCR was performed using specific primers (See Table S1) for *OsIPS1* (A and B), *OsmiR827* (C and D), *OsPT2* (E and F). The expression of wild type under Pi-sufficient condition was set to 1. Values represent means ± standard deviation (SD) of three replicates.

G and H, qRT-PCR analysis of the expression of Pi starvation-responsive genes in the PHR1-3-overepressing plants. RNA from roots and shoots was isolated separately from 20-d-old plants grown in Pi-sufficient (200 μM Pi) solution, and qRT-PCR was performed using specific primers (See Table S1) for *OsIPS1*, *OsmiR827* and *OsPT2*. Asterisks indicate significant differences from WT ($^{*}P < 0.05$, Student's t-test).

Figure 5 Comparative transcriptomes of *phr* mutants

A, Venn diagrams depicting the genes with altered expression in *phr* mutants compared to WT. The total shoot RNA of WT, *phr1*, *phr3*, and *phr1/2/3* seedlings transferred for 7 d to –Pi conditions was isolated for microarray analysis. Three repeat microarrays were performed for each material. The number of transcripts whose expression was higher [mutation (mut) > WT] or lower (mut < WT) in *phr1*, *phr3*, and *phr1*/*2*/*3* plants than in WT plants is shown.

B and C, The number Pi-starvation induced (green bar) or repressed (red bar) genes with altered expression in *phr1*, *phr3* and *phr1/2/3* mutants.

Figure 6 Tissue-specific expression patterns of *OsPHR1*, *OsPHR2* and *OsPHR3*

Tissue-specific expression patterns of *OsPHR1*, *OsPHR2* and *OsPHR3* indicated by expression P_{OsPHR1}:*GUS* (images 1A-1M), P_{OsPHR2}:*GUS* (images 2A-2M) and P_{OsPHR3}:*GUS* (images 3A-3M) fusions in the transgenic plants. In each panel (1-3), images A-C show GUS staining of the primary root: root cap, meristematic zone and elongation zone (C), maturation zone (B,C); Bars in 1-3 = 0.5 mm. (4-5) Cross sections of root elongation zone (D), lateral root (E); Bars = 50 μM. Cross section of GUS-stained leaf blade (F, G); Bars = 100 μm. (H-J) GUS staining of pistil, stamens and shell; (K-M) Cross section at the center of node I. ms: mestome sheath cell, xm: xylem; ph: phloem; sc: sclerenchyma cell; exod, exodermis; ep: epidermis; cor, cortex, st, stele; XL: Xylem region of large vascular bundles; PL: phloem region of large vascular bundles; SV: small vascular bundle; DV: diffuse vascular bundle.

Figure 7 DNA binding properties of PHR1-3

A, Yeast one-hybrid assays of the DNA binding affinity of PHR1-3 for different P1BS types. The variant bases in the P1BS motif of *OsIPS2* were substituted by different bases as indicated; pLacZ2u was used as a negative control.

B, β-galactosidase of activity measurement of PHR1-3 binding to different P1BS versions. Values represent means ± SD of five replicates. Data significantly different from corresponding controls are indicated (Original P1BS versus the substituted P1BS, $^{**}P < 0.01$, Student's t-test).

C, EMSA showing that PHR1-3 preferentially bind to the P1BS GaATATtC (High affinity P1BS, HA-P1BS) rather than GgATATgC (Low affinity P1BS, LA-P1BS). The binding between GST-PHR1-3 and biotin-labeled LA-P1BS was competed by different amounts of unlabeled competitor (HA-P1BS or LA-P1BS). GST protein was used as negative control. The protein amount used was 50 ng per lane, the biotin-labeled DNA probe was 20 fmol per lane. The fold excess of the competitor relative to the labeled probe is indicated above the lane.

D, Relative binding percentage of PHR1-3 competed by increasing amounts of unlabeled HA-P1BS or LA-P1BS, quantified from experiments shown in C. The first lane without competitor was set as 100%.

Figure 8 OsPHR3-overexpressing lines tolerance of Pi stress

A, Growth performance of the wild-type (Nip) and transgenic plants *OsPHR3-Ov-1/8* grown in pots with high-Pi fertilizer (200 mg/kg Pi, HP), moderate-Pi fertilizer (100 mg/kg Pi, MP) and low-Pi fertilizer (30 mg/kg Pi, LP). B and C, the grain yields and numbers of effective panicles per plant; data are means ± SD (n=4); D and E, Total P concentration in shoot and grains; data are means ± SD (n=4). Data significantly different from corresponding controls are indicated ($^{*}P < 0.05$; $^{**}P < 0.01$ Student's t-test).

Figure S1 Phylogram of MYB-CC protein from different species

MYB-CC protein from Arabidopsis (At, Arabidopsis thaliana), rice (Os, Oryza sativa), sorghum (Sb, Sorghum bicolor), maize (GRMZM, Zea mays), millet (Si, Setararia italica), and common wheat (Bradi, Brachypodium distachyon), constructed in MEGA 5.1 using the neighbor-joining method with bootstrap probabilities based on 1000 replicates shown at branch nodes. In addition to the AGI number, names are given for the functionally characterized proteins: PHOSPHATE STARVATION RESPONSE REGULATOR 1 (PHR1) (Rubio et al., 2001); PHR1-LIKE1 (PHL1) (Busto, et al., 2010), OsPHR1 and OsPHR2 (Zhou et al., 2008) and OsPHR3 (this study).

Figure S2 Characterization of Tos-17 insertion mutant of *phr3*

A, Genome structure of OsPHR3 along with the T-DNA insertion position of the phr3 mutant; black boxes denote exons, black lines introns, and white boxes indicate 5' and 3' untranslated regions. The primers R3-F, R3-R and Tos-17-LB used for indentifying phr3 homozygous plants are indicated by arrows. B) PCR identification of the phr3 mutant with the primers of R3-F, R3-R and Tos17-LB; M, DNA marker; C) Semi-quantitative RT-PCR analysis showing the knockout of phr3 mutant. Plants were grown for 15 d in 200 μM Pi solution before harvest for total RNA isolation.

Figure S3 Mutant identification of *phr1*

A, Genome structure of OsPHR1 showing the mutated position in the *phr1* mutant; the red 'CA' are the deleted bases; the bold 'TGA' indicates the stop codon resulting from the 'CA' deletion.

B, The sequencing map of mutated site in WT and the *phr1* mutant; the black box shows the bases deleted in *phr1*.

C, PCR identification of *phr1* mutant with the primers phr1-NcoI-F and phr1-NcoI-R (See Table

S1); the PCR products were digested with restriction endonuclease NcoI and then separated by 10% PAGE.

Figure S4 Identification of OsPHR3-overexpressing lines

A, Necrosis phenotype of three PHR-overexpressing lines under Pi-sufficient conditions (200 μM Pi), the red arrows indicates the necrotic leaves of *OsPHR1-Ov-1* (R1-Ov), *OsPHR2-Ov-1* (R2-*Ov*), *OsPHR3-Ov-1* (R3-Ov-1) and *OsPHR3-Ov-8* (R3-Ov-8).

B, DNA gel blot analysis of wild type (WT) and eight independent transgenic plants of *OsPHR3*-over expressing lines. The DNA gel blots were hybridized to a probe of the hygromycin (HPTII) gene.

CE, Relative mRNA expression of *OsPHR1*, *OsPHR2* and *OsPHR3* in 20-d-old plants of the corresponding overexpression lines under Pi-sufficient conditions (200 μM Pi).

Figure S5 Relative mRNA expression of three PHR genes at different growth stages

Five-day-old wild-type plants were cultured in 200 μM Pi solution, and then the shoot and root were harvested in every 10 d until the plants had grown 70 d. qRT-PCR analysis was used to analyze the relative mRNA expression level at different growth stages. Values represent means ± SD of three replicates. Data significantly different from corresponding controls are indicated (50/60/70-d-old versus other growth stages, $^{**}P < 0.01$; Student's t-test).

Figure S6 Phenotype of PHR2 and PHR3 Flag-tagged lines

A and B, Phenotype performance of PHR2- and PHR3-Flag lines under phosphate-sufficient (HP, 200 μM) and -deficient (LP, 10 μM) conditions, respectively. Three 30-d-old independent transgenic lines of 35S:PHR2-Flag and two lines of 35S:PHR3-Flag were selected for analysis; bar =20 cm. C, Protein expression level in PHR2- and PHR3-Flag lines under phosphate-sufficient conditions. The shown immunoblot was detected using anti-Flag antibody. Equal amounts of protein (15 μg) were used for immunoblotting and staining by Coomassie blue (CBB), indicating similar loading of proteins. D and E, Biomass (D) and Pi concentration (E) of PHR2- and PHR3-Flag lines under phosphate-sufficient (HP, 200 μM) and -deficient (LP, 10 μM) conditions. Values represent means ± SD of six replicates. Significant differences ($^{*}P < 0.05$, $^{**}P < 0.01$) from the wild type (t-test) are indicated.

Figure S7 ***OsPHR3*****-overexpressing plants exhibit low-Pi tolerance under field conditions**

A, Growth performance of OsPHR3-overexpressing lines. The experiment was conducted in long-term nutrient-fixed plots at the Agriculture Experiment Station of Zhejiang University in Changxing county, Zhejiang province, China from May to September in 2014. The control (CK, HP) and moderate fertilizer (MP) plots received 450 kg and 200 kg Ca(H2PO4)2H2O/ha, respectively, before transplanting. No fertilizer was applied to the low-P (LP) plot for four years (from 2009 to 2013). The Soil Olsen P was 3.5 ppm in the low Pi plot, 7.1 ppm in MP and 10.5 ppm in CK. The plants were transplanted at a spacing of 25×25 cm.

B and C, Grain yield and numbers of effective panicles per plant. Data are means ± SD (n =100).

D, 1000-seed weight for WT, *OsPHR3-Ov-1* and *OsPHR3-Ov-8* under HP, MP and LP conditions.

E and F, Total P concentration in shoot and grains; data are means ± SD (n=4).

G, Biomass of WT, *OsPHR3-Ov-1* and *OsPHR3-Ov-8* under HP, MP and LP conditions; data are means ± SD (n=4). Significant difference ($^{*}P < 0.05$, $^{**}P < 0.01$) from the wild type (t-test).

Figure S8 Relative expression of ***OsPHF1*** **and** ***OsPT8*** **in the mutants of** ***phr1/2/3*** **and WT**

Two-week-old plants grown in Pi-sufficient (200 μM Pi) solution were transferred to Pi-sufficient or P-lacking solution for 7 d; RNA from roots and shoots was isolated separately and qRT-PCR was perfromed using specific primers (See Table S1) for *OsPHF1* (A) and *OsPT8* (B).

Figure S9 Root-to-shoot biomass ratio of phr mutants

The 30-d-old seedling root-to-shoot biomass ratios of wild type (WT), *phr1*, *phr2*, *phr3*, *phr1*/*2*, *phr1*/3, *phr2*/3 and *phr1/*2/3 were measured under Pi-sufficient (200 μM Pi) and Pi-deficient (10 μM Pi) hydroponic conditions. Values represent means ±SD of ten replicates.

Figure S10 Relative expression of ***PHR1-PHR3*** **under low-Pi conditions**

Two-week-old plants grown in Pi-sufficient (200 μM Pi) solution were transferred to Pi-sufficient or P-lacking solution for 7d; RNA from roots and shoots was isolated separately and qRT-PCR was performed using specific primers for *PHR1-PHR3* (See Table S1). Values represent means ± SD of three replicates.

707

Integrate regulation of PHR1 subfamily for Pi-signaling and homeostasis in rice

Meina Guo[1ϒ], Wenyuan Ruan[2, 1,ϒ], Changying Li[1], Fangliang Huang[1], Ming Zeng[1], Yingyao Liu[1], Yanan Yu[1], Xiaomeng Ding[1], Yunrong Wu[1], Zhongchang Wu[1], Chuanzao Mao[1], Keke Yi[1, 2], Ping Wu[1], Xiaorong Mo[1]*

Author affiliation:

[1] State Key Laboratory of Plant Physiology and Biochemistry, College of Life Sciences, Zhejiang University, Hangzhou 310058, China.

[2] Institute of Agricultural Resources and Regional Planning, China Academy of Agricultural Sciences, Beijing 100081, China.

ϒ Wenyuan Ruan and Meina Guo contributed equally to this work.

*To whom correspondence should be addressed. E-mail: xiaorong@zju.edu.cn

E-mail of all authors:

Wenyuan Ruan (ruanwenyuan@zju.edu.cn);

Meina Guo (guomeina@zju.edu.cn);

Changying Li (21107015@zju.edu.cn);

Fangliang Huang (huangfl@zju.edu.cn)

Yanan Yu (21207008@zju.edu.cn);

Ming Zeng (21307003@zju.edu.cn);

Yingyao Liu (lyingyao@zju.edu.cn);

Xiaomeng Ding (21307007@zju.edu.cn);

Yunrong Wu (yrwu@zju.edu.cn);

Zhongchang Wu (wzchang@zju.edu.cn);

Chuanzao Mao (mcz@zju.edu.cn) ;

Keke Yi (yikk@zju.edu.cn);

Ping Wu (clspwu@zju.edu.cn)

Xiaorong Mo (xiaorong@zju.edu.cn);

Supplemental Materials

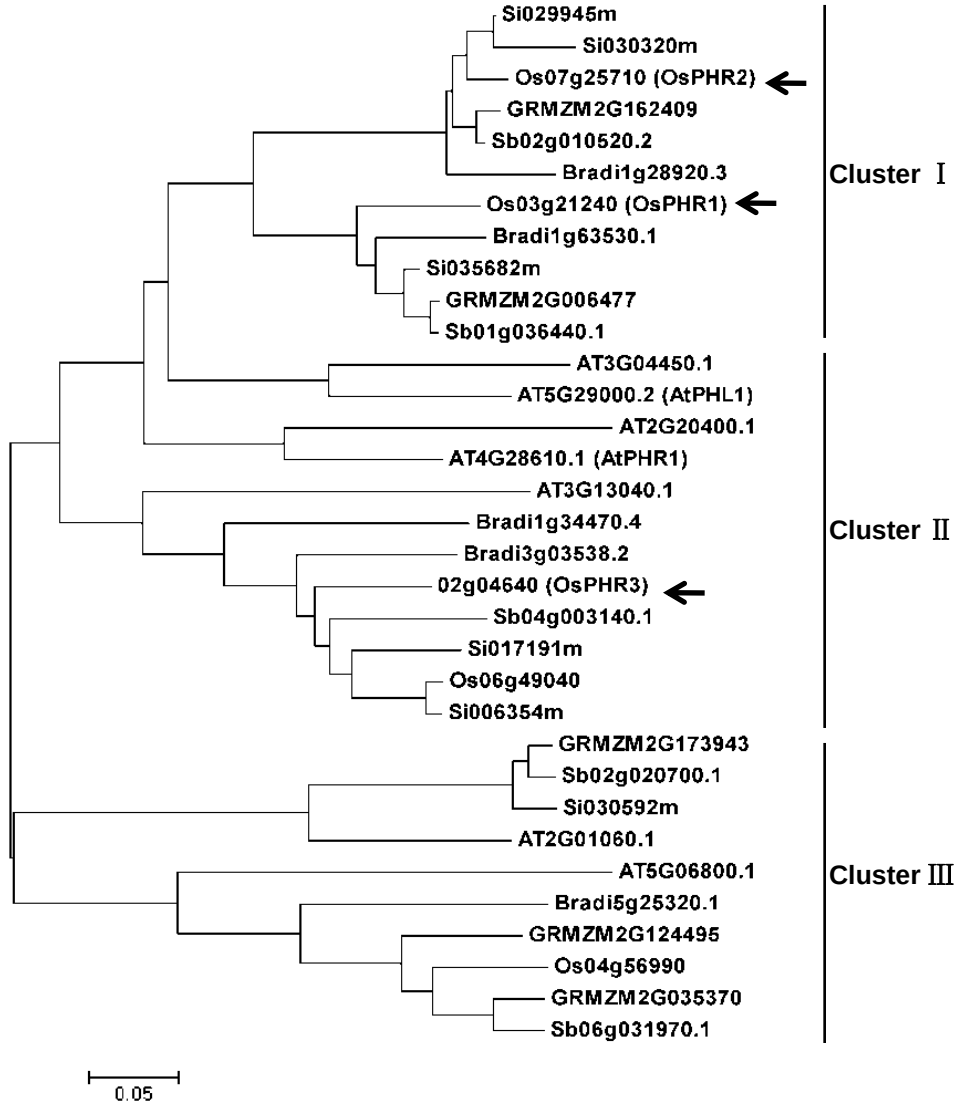

Figure S1 Phylogram of MYB-CC protein from different species

MYB-CC protein from Arabidopsis (At, *Arabidopsis thaliana*), rice (Os, *Oryza sativa*), sorghum (Sb, *Sorghum bicolor*), maize (GRMZM, *Zea mays*), millet (Si, *Setararia italica*), and common wheat (Bradi, *Brachypodium distachyon*), constructed in MEGA 5.1 using the neighbor-joining method with bootstrap probabilities based on 1000 replicates shown at branch nodes. In addition to the AGI number, names are given for the functionally characterized proteins: PHOSPHATE STARVATION RESPONSE REGULATOR 1 (PHR1) (Rubio et al., 2001); PHR1-LIKE1 (PHL1) (Busto, et al., 2010), OsPHR1 and OsPHR2 (Zhou et al., 2008) and OsPHR3 (this study).

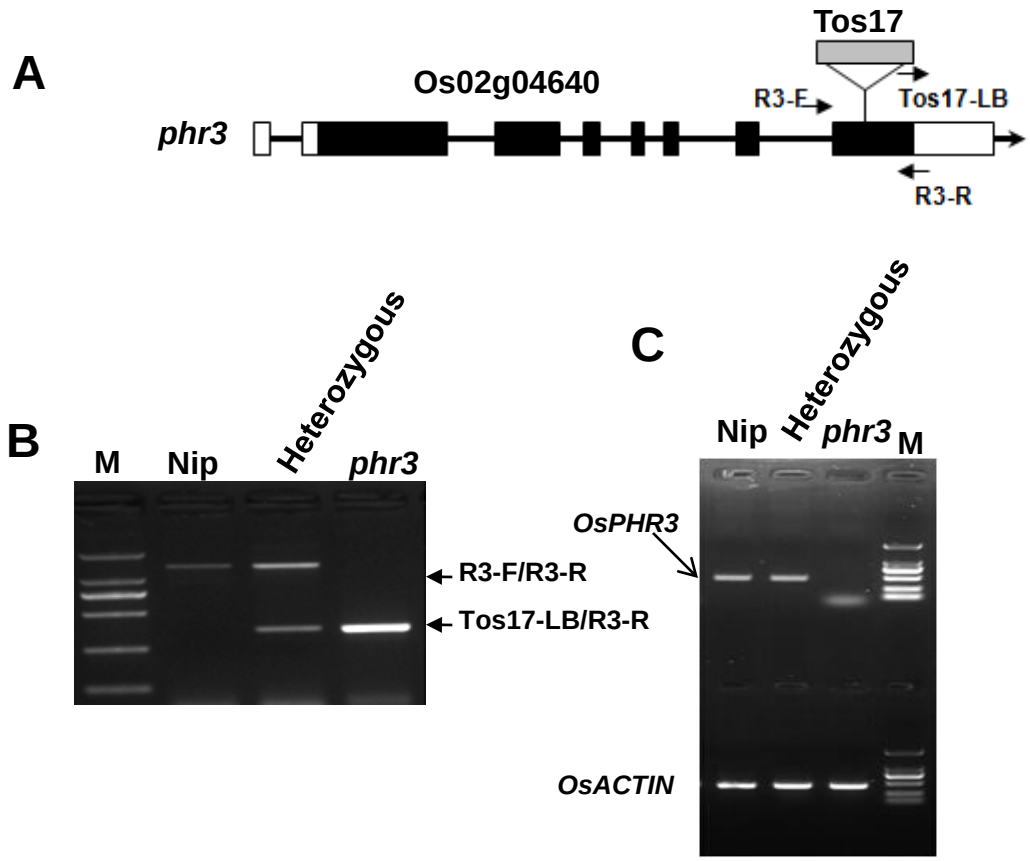

Figure S2 Characterization of Tos-17 insertion mutant of *phr3*

A, Genome structure of *OsPHR3* along with the T-DNA insertion position of the *phr3* mutant; black boxes denote exons, black lines introns, and white boxes indicate 5' and 3' untranslated regions. The primers R3-F, R3-R and Tos-17-LB used for indentifying *phr3* homozygous plants are indicated by arrows. B) PCR identification of the *phr3* mutant with the primers of R3-F, R3-R and Tos17-LB; M, DNA marker; C) Semi-quantitative RT-PCR analysis showing the knockout of *phr3* mutant. Plants were grown for 15 d in 200 μM Pi solution before harvest for total RNA isolation.

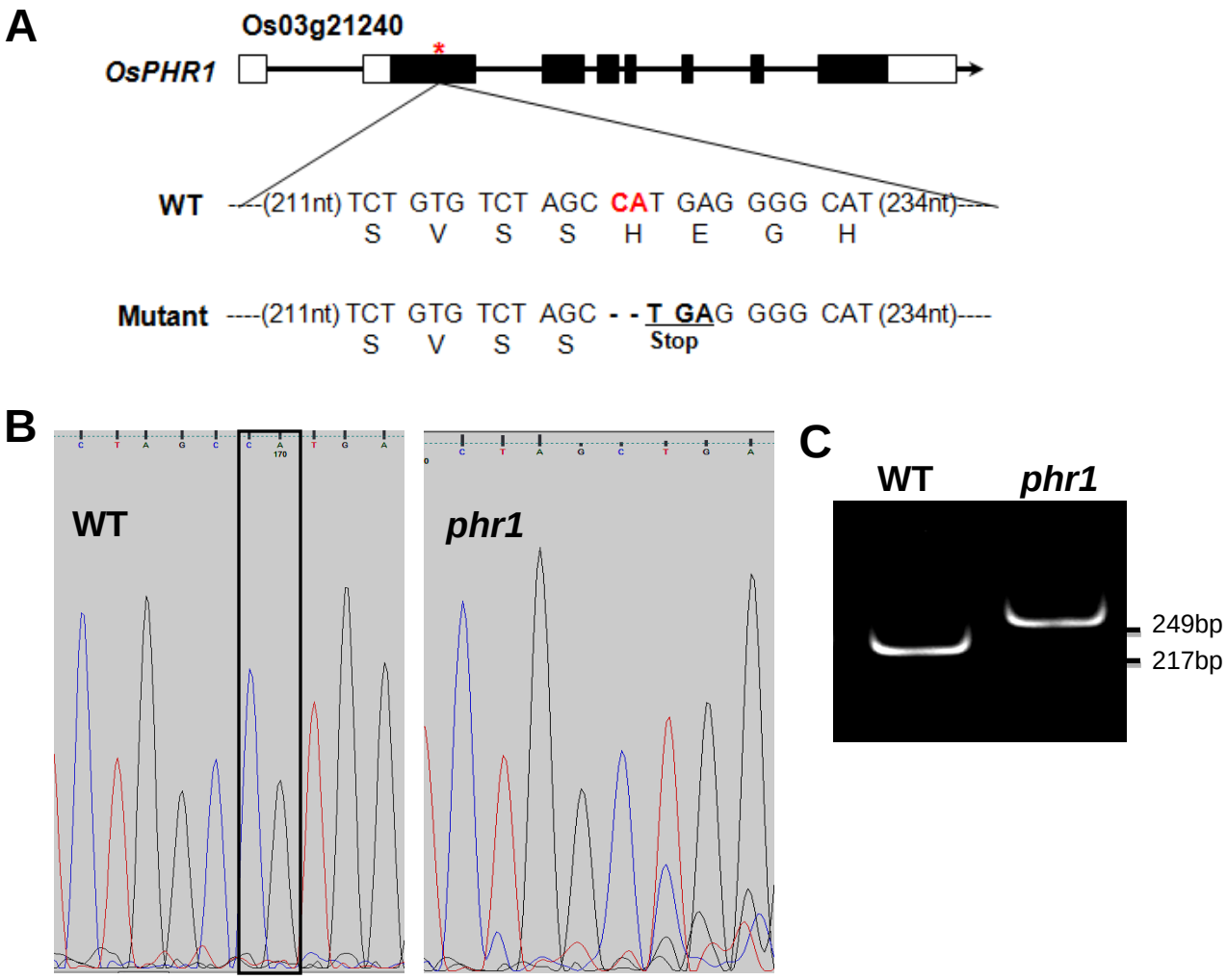

Figure S3 Mutant identification of *phr1*

A, Genome structure of *OsPHR1* showing the mutated position in the *phr1* mutant; the red 'CA' are the deleted bases; the bold 'TGA' indicates the stop codon resulting from the 'CA' deletion.

B, The sequencing map of mutated site in WT and the *phr1* mutant; the black box shows the bases deleted in *phr1*.

C, PCR identification of *phr1* mutant with the primers *phr1*-NcoI-F and *phr1*-NcoI-R (**See Table S1**); the PCR products were digested with restriction endonuclease NcoI and then separated by 10% PAGE.

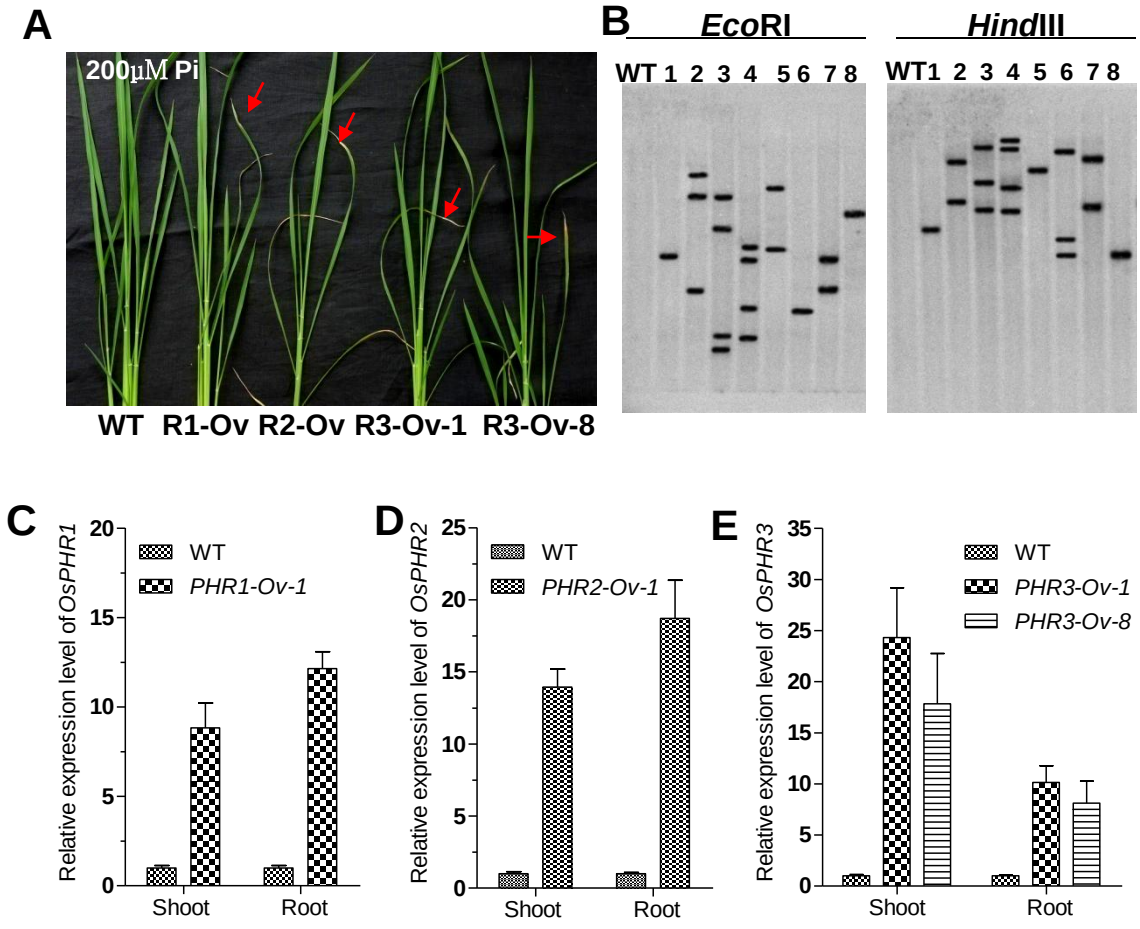

Figure S4 Identification of *OsPHR3*-overexpressing lines

A, Necrosis phenotype of three PHR-overexpressing lines under Pi-sufficient conditions (200 μM Pi), the red arrows indicates the necrotic leaves of *OsPHR1-Ov-1* (R1-Ov), *OsPHR2-Ov-1* (R2-Ov), *OsPHR3-Ov-1* (R3-Ov-1) and *OsPHR3-Ov-8* (R3-Ov-8).

B, DNA gel blot analysis of wild type (WT) and eight independent transgenic plants of *OsPHR3*-over expressing lines. The DNA gel blots were hybridized to a probe of the *hygromycin* (*HPTII*) gene.

C –E, Relative mRNA expression of *OsPHR1*, *OsPHR2* and *OsPHR3* in 20-d-old plants of the corresponding overexpression lines under Pi-sufficient conditions (200 μM Pi).

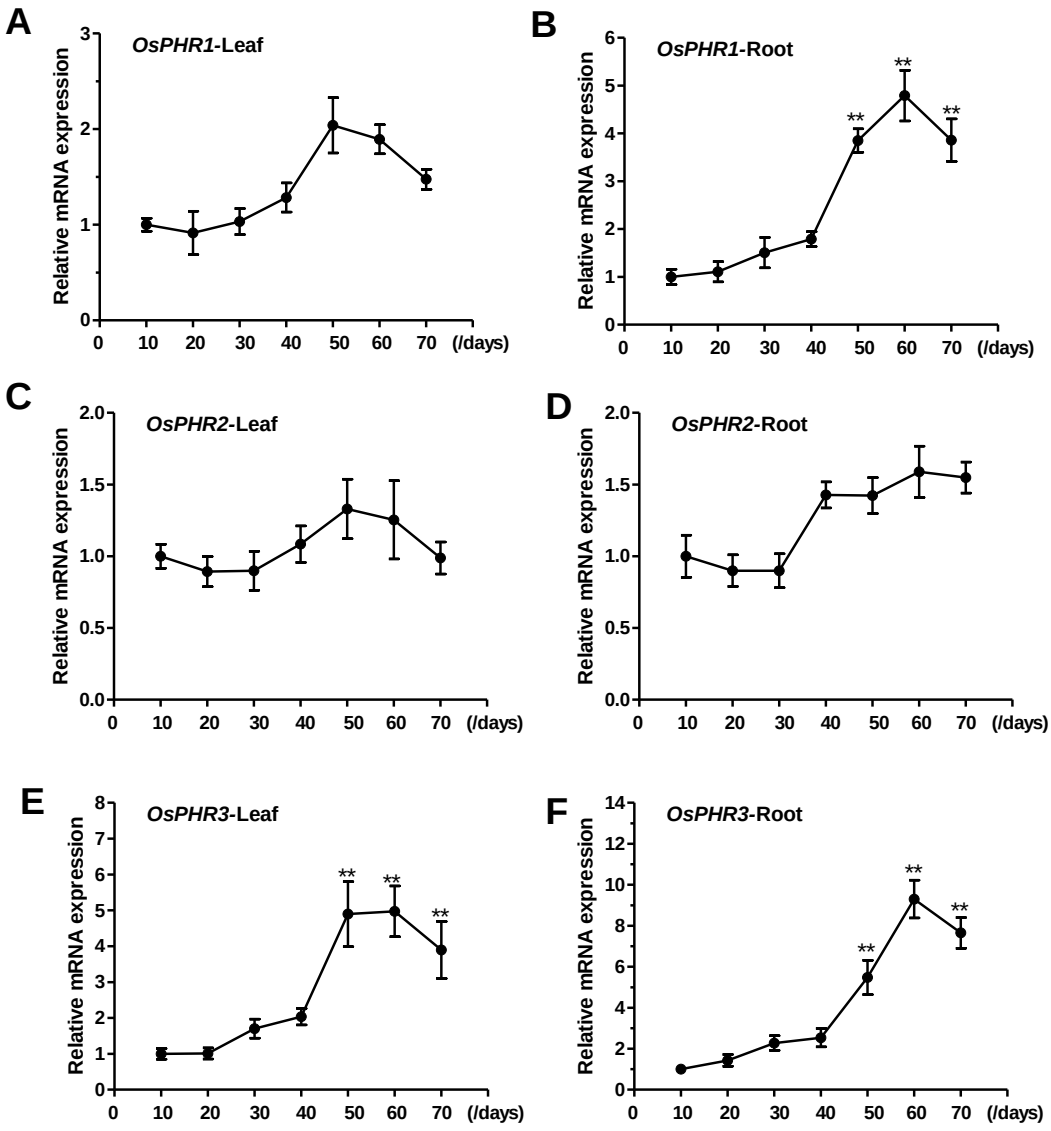

Figure S5 Relative mRNA expression of three *PHR* genes at different growth stages

Five-day-old wild-type plants were cultured in 200 μM Pi solution, and then the shoot and root were harvested in every 10 d until the plants had grown 70 d. qRT-PCR analysis was used to analyze the relative mRNA expression level at different growth stages. Values represent means ± SD of three replicates. Data significantly different from corresponding controls are indicated (50/60/70-d-old versus other growth stages, $^{**}p < 0.01$; Student's *t*-test).

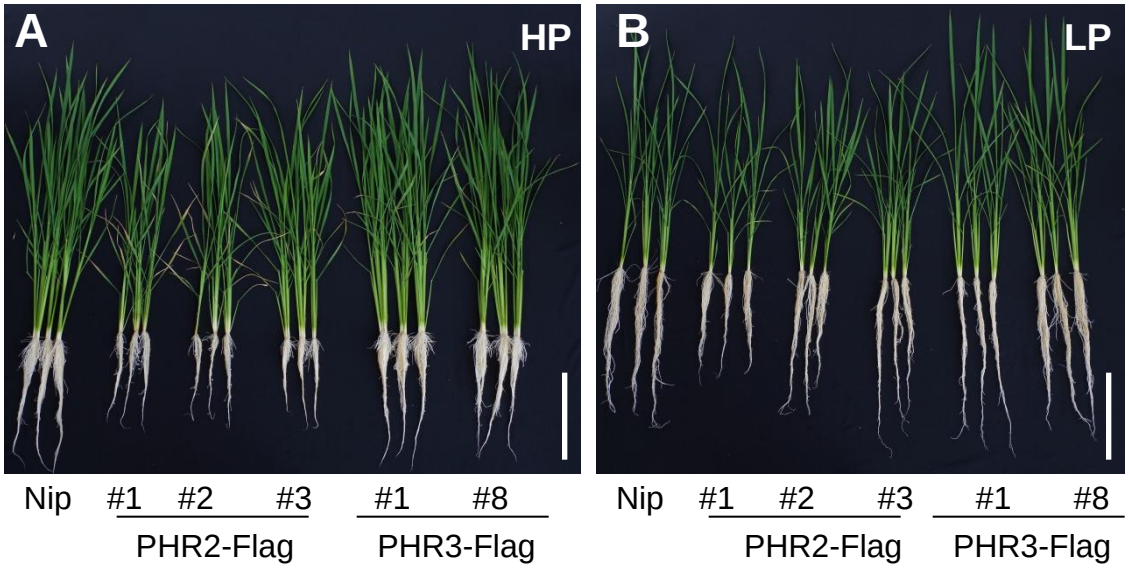

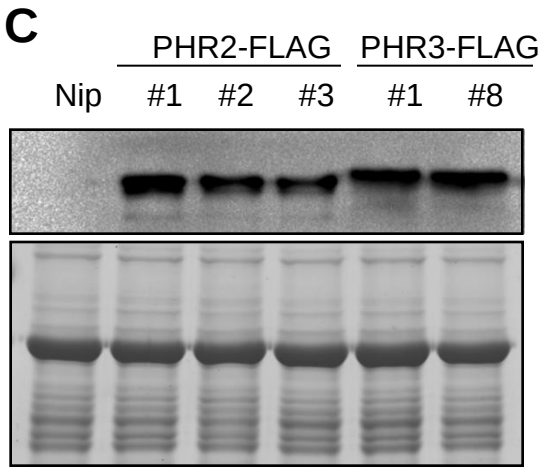

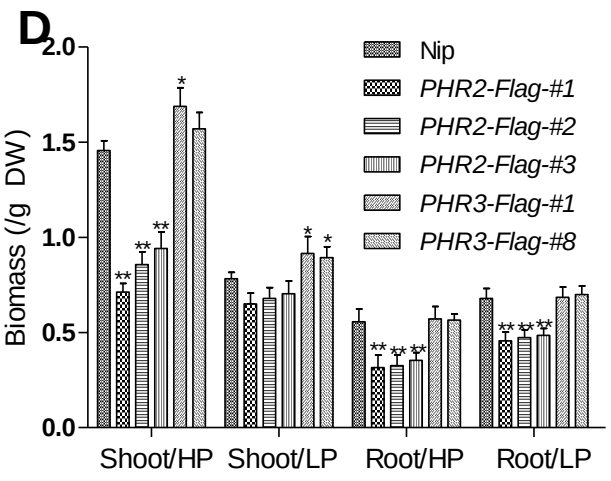

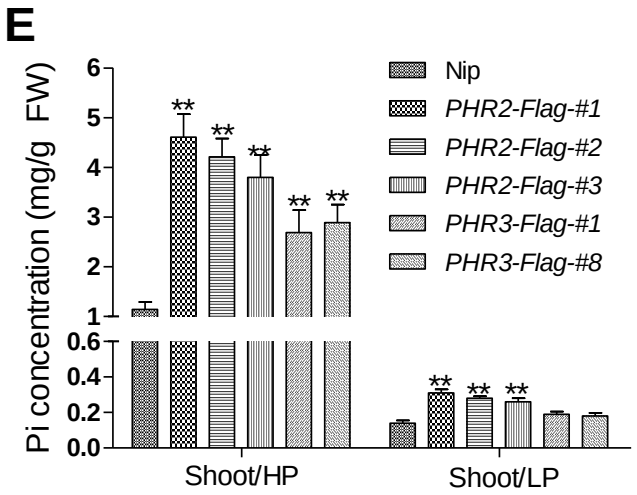

Figure S6 Phenotype of PHR2 and PHR3 Flag-tagged lines

A and B, Phenotype performance of PHR2- and PHR3-Flag lines under phosphate-sufficient (HP, 200 μM) and -deficient (LP, 10 μM) conditions, respectively. Three 30-d-old independent transgenic lines of 35S:PHR2-Flag and two lines of 35S:PHR3-Flag were selected for analysis; bar =20 cm. C, Protein expression level in PHR2- and PHR3-Flag lines under phosphate-sufficient conditions. The shown immunoblot was detected using anti-Flag antibody. Equal amounts of protein (15 μg) were used for immunoblotting and staining by Coomassie blue (CBB), indicating similar loading of proteins. D and E, Biomass (D) and Pi concentration (E) of PHR2- and PHR3-Flag lines under phosphate-sufficient (HP, 200 μM) and -deficient (LP, 10 μM) conditions. Values represent means ± SD of six replicates. Significant differences ($^{*}P < 0.05$, $^{**}P < 0.01$) from the wild type (t-test) are indicated.

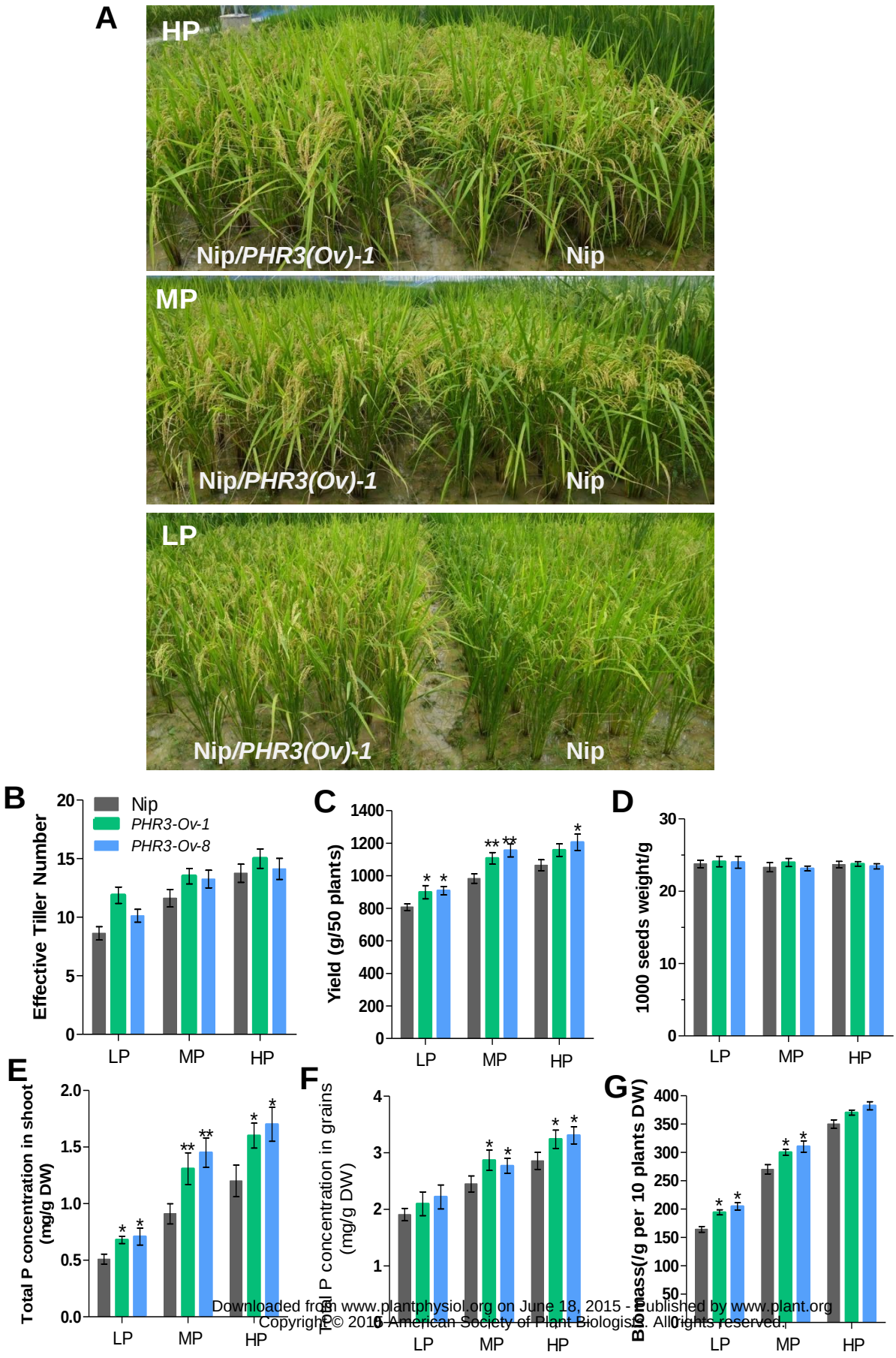

Figure S7 *OsPHR3*-overexpressing plants exhibit low-Pi tolerance under field conditions

A, Growth performance of *OsPHR3*-overexpressing lines. The experiment was conducted in long-term nutrient-fixed plots at the Agriculture Experiment Station of Zhejiang University in Changxing county, Zhejiang province, China from May to September in 2014. The control (CK, HP) and moderate fertilizer (MP) plots received 450 kg and 200 kg $Ca(H_2PO_4)_2H_2O$/ha, respectively, before transplanting. No fertilizer was applied to the low-P (LP) plot for four years (from 2009 to 2013). The Soil Olsen P was 3.5 ppm in the low Pi plot, 7.1 ppm in MP and 10.5 ppm in CK. The plants were transplanted at a spacing of 25×25 cm.

B and C, Grain yield and numbers of effective panicles per plant. Data are means ± SD (n =100).

D, 1000-seed weight for WT, *OsPHR3-Ov-1* and *OsPHR3-Ov-8* under HP, MP and LP conditions.

E and F, Total P concentration in shoot and grains; data are means ± SD (n=4).

G, Biomass of WT, *OsPHR3-Ov-1* and *OsPHR3-Ov-8* under HP, MP and LP conditions; data are means ± SD (n=4). Significant difference (* $P < 0.05$, ** $P < 0.01$) from the wild type (*t*-test).

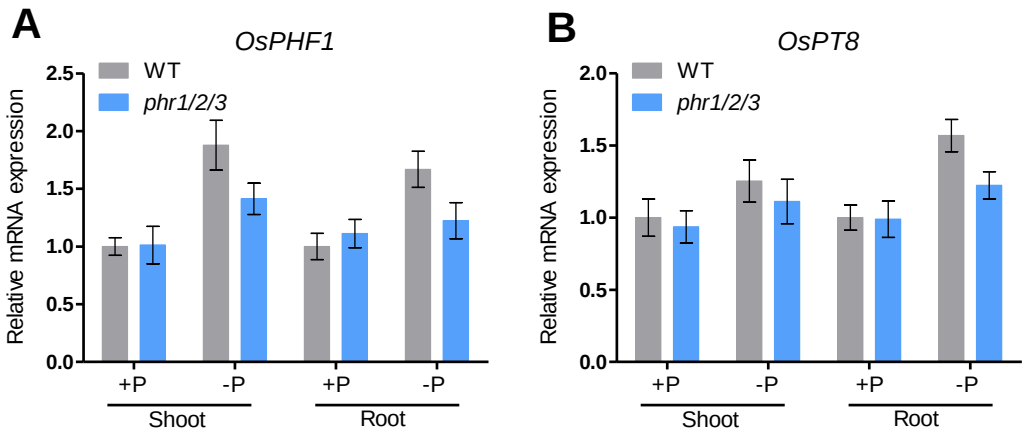

Figure S8 Relative expression of *OsPHF1* and *OsPT8* in the mutants of *phr1/2/3* and WT

Two-week-old plants grown in Pi-sufficient (200 μM Pi) solution were transferred to Pi-sufficient or P-lacking solution for 7 d; RNA from roots and shoots was isolated separately and qRT-PCR was perfromed using specific primers (**See Table S1**) for *OsPHF1* (A) and *OsPT8* (B).

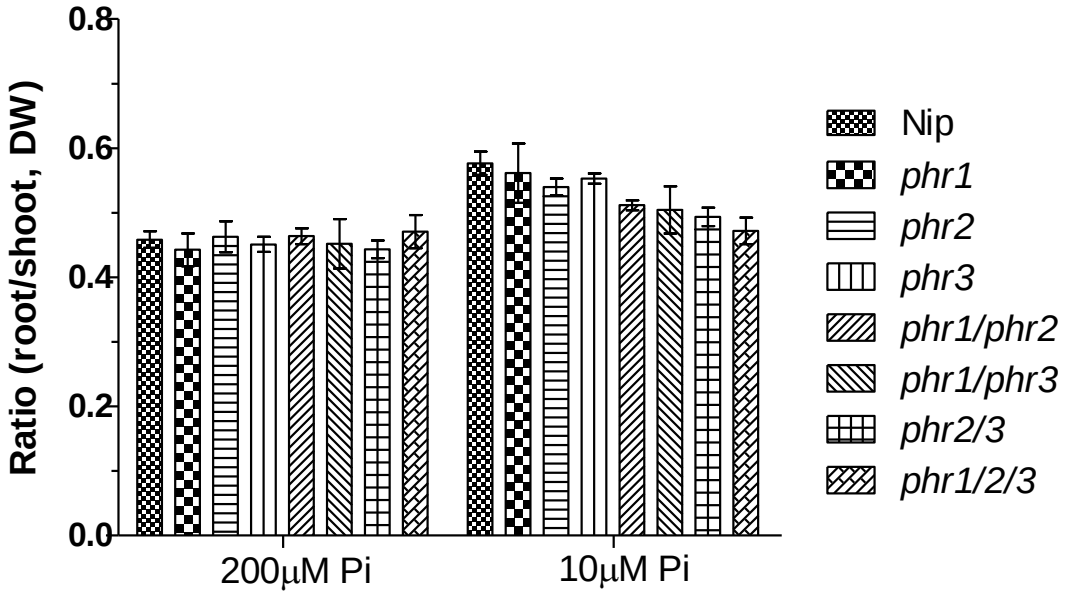

Figure S9 Root-to-shoot biomass ratio of *phr* mutants

The 30-d-old seedling root-to-shoot biomass ratios of wild type (WT), *phr1*, phr2, *phr3*, *phr1/2*, *phr1/3*, *phr2/3* and *phr1/2/3* were measured under Pi-sufficient (200 μM Pi) and Pi-deficient (10 μM Pi) hydroponic conditions. Values represent means ±SD of ten replicates.

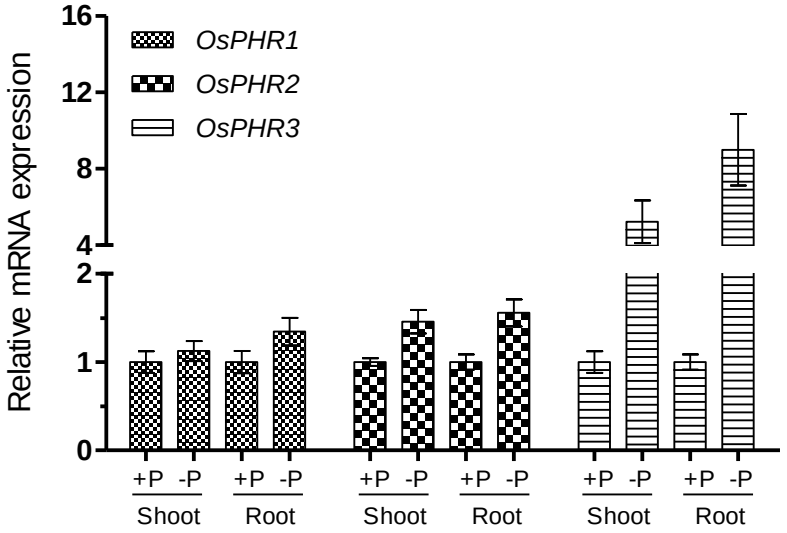

Figure S10 Relative expression of *PHR1-3* under low-Pi conditions

Two-week-old plants grown in Pi-sufficient (200 μM Pi) solution were transferred to Pi-sufficient or P-lacking solution for 7d; RNA from roots and shoots was isolated separately and qRT-PCR was performed using specific primers for *PHR1-3* (**See Table S1**). Values represent means ± SD of three replicates.

Parsed Citations

Bari R, Datt PB, Stitt M, Scheible W (2006) PHO2, microRNA399 and PHR1 define a phosphate-signaling pathway in plants. Plant Physiol 141: 988-999
Pubmed: Author and Title
CrossRef: Author and Title
Google Scholar: Author Only Title Only Author and Title

Bayle V, Arrighi JF, Creff A, Nespoulous C, Vialaret J, Rossignol M, Gonzalez E, Paz-Ares J, Nussaume L (2011) Arabidopsis thaliana high-af?nity phosphate transporters exhibit multiple levels of posttranslational regulation. Plant Cell 23:1523-1535
Pubmed: Author and Title
CrossRef: Author and Title
Google Scholar: Author Only Title Only Author and Title

Boter M, Rui´z-Rivero O, Abdeen A, Prat S (2004) Conserved MYC transcription factors play a key role in jasmonate signaling both in tomato and Arabidopsis. Genes Dev 18: 1577-1591
Pubmed: Author and Title
CrossRef: Author and Title
Google Scholar: Author Only Title Only Author and Title

Bournier M, Tissot N, Mari S, Boucherez J, Lacombe E, Briat JF, Gaymard F (2013) Arabidopsis ferritin 1 (AtFer1) gene regulation by the phosphate starvation response 1 (AtPHR1) transcription factor reveals a direct molecular link between iron and phosphate homeostasis. J Biol Chem 288:22670-22680
Pubmed: Author and Title
CrossRef: Author and Title
Google Scholar: Author Only Title Only Author and Title

Bustos R, Castrillo G, Linhares F, Puga MI, Rubio V, Perez-Perez J, Solano R, Leyva A, Paz-Ares J (2010) A central regulatory system largely controls transcriptional activation and repression responses to phosphate starvation in Arabidopsis. PLoS Genet 6: e1001102
Pubmed: Author and Title
CrossRef: Author and Title
Google Scholar: Author Only Title Only Author and Title

Carroll D (2012) A CRISPR approach to gene targeting. Mol Ther 20: 1658-1660
Pubmed: Author and Title
CrossRef: Author and Title
Google Scholar: Author Only Title Only Author and Title

Chen JY, Liu Y, Ni J, Wang YF, Bai YH, Shi J, Gan J, Wu ZC, Wu P (2011) OsPHF1 regulates the plasma membrane localization of low- and high-affinity inorganic phosphate transporters and determines inorganic phosphate uptake and translocation in Rice. Plant Physiol 157: 269-278
Pubmed: Author and Title
CrossRef: Author and Title
Google Scholar: Author Only Title Only Author and Title

Chen S, Jin W, Wang M, Zhang F, Zhou J, Jia Q, Wu Y, Liu F, Wu P (2003) Distribution and characterization of over 1000 T-DNA tags in rice genome. Plant J. 36:105-113
Pubmed: Author and Title
CrossRef: Author and Title
Google Scholar: Author Only Title Only Author and Title

Chiou TJ, Lin SI (2011) Signaling network in sensing phosphate availability in plants. Anu Rev Plant Biol 62:185-206
Pubmed: Author and Title
CrossRef: Author and Title
Google Scholar: Author Only Title Only Author and Title

Devoto A, Ellis C, Magusin A, Chang H-S, Chilcott C, Zhu T, Turner J G (2005) Expression profiling reveals COI1 to be a key regulator of genes involved in wound- and methyl jasmonate-induced secondary metabolism, defence, and hormone interactions. Plant Mol Biol 58: 497-513
Pubmed: Author and Title
CrossRef: Author and Title
Google Scholar: Author Only Title Only Author and Title

Dombrecht B, Xue GP, Sprague SJ, Kirkegaard JA, Ross JJ, Reid JB, Fitt GP, Sewelam N, Schenk PM, Manners JM, Kazan K (2007) MYC2 differentially modulates diverse jasmonate-dependent functions in Arabidopsis. Plant Cell 19:2225-2245
Pubmed: Author and Title
CrossRef: Author and Title
Google Scholar: Author Only Title Only Author and Title

Feng ZY, Mao YF, Xu NF, Zhang BT, Wei PL, Yang DL, Wang Z, Zhang ZJ, Zheng R, Yang L, Zeng L, Liu XD, Zhu JK (2014) Multigeneration analysis reveals the inheritance, specificity, and patterns of CRISPR/Cas-induced gene modifications in Arabidopsis. PNAS 111: 4632-4637
Pubmed: Author and Title
CrossRef: Author and Title
Google Scholar: Author Only Title Only Author and Title

Feng ZY, Zhang BT, Ding WN, Liu XD, Yang DL Wei PL, Cao FQ, Zhu SH, Zhang F, Mao YF, Zhu JK (2013) Efficient genome editing in plants using a CRISPR/Cas system. Cell Research 23:1229-1232

Pubmed: Author and Title
CrossRef: Author and Title
Google Scholar: Author Only Title Only Author and Title

Fernández-Calvo P, Chini A, Fernández-Barbero G, Chico JM, Gimenez-Ibanez S, Geerinck J, Eeckhout D, Schweizer F, Godoy M, Franco-Zorrilla JM, Pauwels L, Witters E, Puga MI, Paz-Ares J, Goossens A, Reymond P, De Jaeger G, Solano R (2011) The Arabidopsis bHLH transcription factors MYC3 and MYC4 are targets of JAZ repressors and act additively with MYC2 in the activation of jasmonate responses. Plant Cell 23:701-715

Pubmed: Author and Title
CrossRef: Author and Title
Google Scholar: Author Only Title Only Author and Title

Franco-Zorrilla JM, Gonza´lez E, Bustos R, Linhares F, Leyva A, Paz-Ares J (2004) The transcriptional control of plant responses to phosphate limitation. J Exp Bot 55: 285-293

Pubmed: Author and Title
CrossRef: Author and Title
Google Scholar: Author Only Title Only Author and Title

Franco-Zorrilla JM, Valli A, Todesco M, Mateos I, Puga MI, Rubio-Somoza I, Leyva A, Weigel D, García JA, Paz-Ares J (2007) Target mimicry provides a new mechanism for regulation of microRNA activity. Nat Genet 39: 1033-1037

Pubmed: Author and Title
CrossRef: Author and Title
Google Scholar: Author Only Title Only Author and Title

Goff, S.A., Ricke, D., Lan, T.H., Presting, G., Wang, R., Dunn, M., Glazebrook, J., Sessions, A., Oeller, P., Varma, H., Hadley, D., Hutchison, D., Martin, C., Katagiri, F., Lange, B.M., Moughamer, T., Xia, Y., Budworth, P., Zhong, J., Miguel, T., Paszkowski, U., Zhang, S., Colbert, M., Sun, W.L., Chen, L., Cooper, B., Park, S., Wood, T.C., Mao, L., Quail, P., Wing, R., Dean, R., Yu, Y., Zharkikh, A., Shen, R., Sahasrabudhe, S., Thomas, A., Cannings, R., Gutin, A., Pruss, D., Reid, J., Tavtigian, S., Mitchell, J., Eldredge, G., Scholl, T., Miller, R.M., Bhatnagar, S., Adey, N., Rubano, T., Tusneem, N., Robinson, R., Feldhaus, J., Macalma, T., Oliphant, A., and Briggs, S. (2002). A draft sequence of the rice genome (Oryza sativa L. ssp. japonica). Science 296, 92-100

Pubmed: Author and Title
CrossRef: Author and Title
Google Scholar: Author Only Title Only Author and Title

González E, Solano R, Rubio V, Leyva A, Paz-Ares J (2005) PHOSPHATE TRANSPORTER TRAFFIC FACILITATOR1 is a plant-specific SEC12-related protein that enables the endoplasmic reticulum exit of a high-affinity phosphate transporter in Arabidopsis. Plant Cell 17: 3500-3512

Pubmed: Author and Title
CrossRef: Author and Title
Google Scholar: Author Only Title Only Author and Title

Hale CR, Zhao P, Olson S, Duff MO, Graveley BR, Wells L, Terns RM, Terns MP (2009)RNA-guided RNA cleavage by a CRISPR RNA-Cas protein complex. Cell 139:945-956

Pubmed: Author and Title
CrossRef: Author and Title
Google Scholar: Author Only Title Only Author and Title

Hinsinger P, Betencourt E, Bernard L, Brauman A, Plassard C, Shen J, Tang X, Zhang F (2011) P for two, sharing a scarce resource: soil phosphorus acquisition in the rhizosphere of intercropped species. Plant Physiol 156:1078-1086

Pubmed: Author and Title
CrossRef: Author and Title
Google Scholar: Author Only Title Only Author and Title

Hsieh LC, Lin SI, Shih ACC, Chen JW, Lin WY, Tseng CY, Li WH, Chiou TJ (2009) Uncovering small rna-mediated responses to phosphate deficiency in Arabidopsis by deep sequencing. Plant Physiol 151:2120-2132

Pubmed: Author and Title
CrossRef: Author and Title
Google Scholar: Author Only Title Only Author and Title

Hu B, Zhu C, Li F, Tang J, Wang Y, Lin A, Liu L, Che R, Chu C (2011) LEAF TIP NECROSIS1 plays a pivotal role in regulation of multiple phosphate starvation responses in rice. Plant Physiol 156:1101-1115

Pubmed: Author and Title
CrossRef: Author and Title
Google Scholar: Author Only Title Only Author and Title

Huang TK, Han CL, Lin SI, Chen YJ, Tsai YC, Chen YR, Chen JW, Lin WY, Chen PM, Liu TY, Chen YS, Sun CM, Chiou TJ (2013) Identification of downstream components of ubiquitin-conjugating enzyme PHOSPHATE2 by quantitative membrane proteomics in Arabidopsis roots. Plant Cell 25: 4044-4060

Pubmed: Author and Title
CrossRef: Author and Title
Google Scholar: Author Only Title Only Author and Title

Jefferson RA, Karanagh TA, Bevan MW (1987) GUS fusion: ß-Glucuronidase as a sensitive and versatile gene fusion marker in higher plants. EMBO J 6: 3901-3907

Pubmed: Author and Title
CrossRef: Author and Title
Google Scholar: Author Only Title Only Author and Title

Jia H, Ren H, Gu M, Zhao J, Sun S, Zhang X, Chen J, Wu P, Xu G (2011) The phosphate transporter gene OsPht1;8 is involved in phosphate homeostasis in rice. Plant Physiol 156:1164-1175

Pubmed: Author and Title
CrossRef: Author and Title
Google Scholar: Author Only Title Only Author and Title

Jinek M, Chylinski K, Fonfara I, Hauer M, Doudna JA, Charpentier E (2012) A programmable dual-RNA-guided DNA endonuclease in adaptive bacterial immunity. Science 337:816-821
Pubmed: Author and Title
CrossRef: Author and Title
Google Scholar: Author Only Title Only Author and Title

Jore MM, Lundgren M, van Duijn E, Bultema JB, Westra ER, Waghmare SP, Wiedenheft B, Pul U, Wurm R, Wagner R, Beijer MR, Barendregt A, Zhou K, Snijders AP, Dickman MJ, Doudna JA, Boekema EJ, Heck AJ, van der Oost J, Brouns SJ (2011) Structural basis for CRISPR RNA-guided DNA recognition by Cascade. Nat Struct Mol Biol 18:529-536
Pubmed: Author and Title
CrossRef: Author and Title
Google Scholar: Author Only Title Only Author and Title

Kant S, Peng M, Rothstein SJ (2011) Genetic regulation by NLA and microRNA827 for maintaining nitrate-dependent phosphate homeostasis in Arabidopsis. PLoS Genet 7: e1002021
Pubmed: Author and Title
CrossRef: Author and Title
Google Scholar: Author Only Title Only Author and Title

Klecker M, Gasch P, Peisker H, Dörmann P, Schlicke H, Grimm B, Mustroph A (2014) A Shoot-Specific Hypoxic Response of Arabidopsis Sheds Light on the Role of the Phosphate-Responsive Transcription Factor PHOSPHATE STARVATION RESPONSE1. Plant Physiol 165:774-790
Pubmed: Author and Title
CrossRef: Author and Title
Google Scholar: Author Only Title Only Author and Title

Lin SI, Santi C, Jobet E, Lacut E, El Kholti N, Karlowski WM, Verdeil JL, Breitler JC, Périn C, Ko SS, Guiderdoni E, Chiou TJ, Echeverria M (2010) Complex regulation of two target genes encoding SPX-MFS proteins by rice miR827 in response to phosphate starvation. Plant and Cell Physiology 51:2119-2131
Pubmed: Author and Title
CrossRef: Author and Title
Google Scholar: Author Only Title Only Author and Title

Lin WY, Huang TK, Chiou TJ (2013) NITROGEN LIMITATION ADAPTATION, a Target of MicroRNA827, mediates degradation of plasma membrane-localized phosphate transporters to maintain phosphate homeostasis in Arabidopsis. Plant Cell 113: 116012
Pubmed: Author and Title
CrossRef: Author and Title
Google Scholar: Author Only Title Only Author and Title

Liu F, Wang ZY, Ren HY, Shen CJ, Li Y, Ling HQ, Wu CY, Lian XM, Wu P (2010) OsSPX1 suppresses the function of OsPHR2 in the regulation of expression of OsPT2 and phosphate homeostasis in shoots of rice. Plant J 62: 508-517
Pubmed: Author and Title
CrossRef: Author and Title
Google Scholar: Author Only Title Only Author and Title

Lorenzo O, Chico JM, Sa´nchez-Serrano JJ, Solano R (2004) JASMONATE-INSENSITIVE1 encodes a MYC transcription factor essential to discriminate between different jasmonate-regulated defense responses in Arabidopsis. Plant Cell 16:1938-1950
Pubmed: Author and Title
CrossRef: Author and Title
Google Scholar: Author Only Title Only Author and Title

Lv QD, Zhong YJ, Wang YG, Wang ZY, Zhang L, Shi J, Wu ZC, Liu Y, Mao CZ, Yi KK, Wu P (2014) SPX4 Negatively Regulates Phosphate Signaling and Homeostasis through Its Interaction with PHR2 in Rice. Plant Cell 26: 1586-1597
Pubmed: Author and Title
CrossRef: Author and Title
Google Scholar: Author Only Title Only Author and Title

Mao Y, Zhang H, Xu N, Zhang B, Gou F, Zhu JK (2013) Application of the CRISPR-Cas system for efficient genome engineering in plants. Mol Plant 6:2008-2011
Pubmed: Author and Title
CrossRef: Author and Title
Google Scholar: Author Only Title Only Author and Title

Martín AC, Del Pozo JC, Iglesias J, Rubio V, Solano R, De La Peña A, Leyva A, Paz-Ares J. (2000) Influence of cytokinins on the expression of phosphate starvation responsive genes in Arabidopsis. Plant J 24: 559-567
Pubmed: Author and Title
CrossRef: Author and Title
Google Scholar: Author Only Title Only Author and Title

Miura K, Rus A, Sharkhuu A, Yokoi S, Karthikeyan AS, Raghothama KG, Baek D, Koo YD, Jin JB, Bressan RA, Yun DJ, Hasegawa PM (2005) The Arabidopsis SUMO E3 ligase SIZ1 controls phosphate deficiency responses. Proc Natl Acad Sci 102: 7760-7765
Pubmed: Author and Title
CrossRef: Author and Title
Google Scholar: Author Only Title Only Author and Title

Nilsson L, Lundmark M, Jensen PE, Nielsen TH (2012) The Arabidopsis transcription factor PHR1 is essential for adaptation to

high light and retaining functional photosynthesis during phosphate starvation. Physiol Plant 144:35-47
Pubmed: Author and Title
CrossRef: Author and Title
Google Scholar: Author Only Title Only Author and Title

Nilsson L, Müller R, Nielsen TH (2007) Increased expression of the MYB-related transcription factor, PHR1, leads to enhanced phosphate uptake in Arabidopsis thaliana. Plant Cell Environ 30:1499-1512
Pubmed: Author and Title
CrossRef: Author and Title
Google Scholar: Author Only Title Only Author and Title

Park BS, Seo JS, Chua NH (2014) NITROGEN LIMITATION ADAPTATION recruits PHOSPHATE2 to target the phosphate transporter PT2 for degradation during the regulation of Arabidopsis phosphate homeostasis. Plant Cell 26:454-64
Pubmed: Author and Title
CrossRef: Author and Title
Google Scholar: Author Only Title Only Author and Title

Paszkowski U, Kroken S, Roux C, Briggs SP (2002) Rice phosphate transporters include an evolutionarily divergent gene specifically activated in arbuscular mycorrhizal symbiosis. PNAS 99:13324-13329
Pubmed: Author and Title
CrossRef: Author and Title
Google Scholar: Author Only Title Only Author and Title

Peng M, Hannam C, Gu H, Bi YM, Rothstein SJ (2007) A mutation in NLA, which encodes a RING-type ubiquitin ligase, disrupts the adaptability of Arabidopsis to nitrogen limitation. Plant J 50:320-337
Pubmed: Author and Title
CrossRef: Author and Title
Google Scholar: Author Only Title Only Author and Title

Puga MI, Mateos I, Charukesi R, Wang Z, Franco-Zorrilla JM, de Lorenzo L, Irigoyen ML, Masiero S, Bustos R, Rodríguez J, Leyva A, Rubio V, Sommer H, Paz-Ares J (2014) SPX1 is a phosphate-dependent inhibitor of PHOSPHATE STARVATION RESPONSE 1 in Arabidopsis. Proc Natl Acad Sci 111: 14947-14952
Pubmed: Author and Title
CrossRef: Author and Title
Google Scholar: Author Only Title Only Author and Title

Rajkumar AS, Dénervaud N, Maerkl SJ. (2013). Mapping the fine structure of a eukaryotic promoter input-output function. Nat Genet. 45: 1207-1215.
Pubmed: Author and Title
CrossRef: Author and Title
Google Scholar: Author Only Title Only Author and Title

Ren F, Guo QQ, Chang LL, Chen L, Zhao CZ, Zhong H, Li XB (2012) Brassica napus PHR1 gene encoding a MYB-like protein functions in response to phosphate starvation. PLoS ONE 7: e44005
Pubmed: Author and Title
CrossRef: Author and Title
Google Scholar: Author Only Title Only Author and Title

Rouached H, Arpat AB, Poirier Y (2010) Regulation of phosphate starvation responses in plants: signaling players and cross-talks. Mol Plant 3:288-299
Pubmed: Author and Title
CrossRef: Author and Title
Google Scholar: Author Only Title Only Author and Title

Rouached H, Secco D, Arpat AB, Poirier Y (2011a) The transcription factor PHR1 plays a key role in the regulation of sulfate shoot-to-root flux upon phosphate starvation in Arabidopsis. BMC Plant Biol 11: 19
Pubmed: Author and Title
CrossRef: Author and Title
Google Scholar: Author Only Title Only Author and Title

Ruan WY, Guo MN, Cai LL, Hu HT, Li CY, Yu Liu, Wu ZC, Mao CZ, Yi KK, Wu P, Mo XR (2015) Genetic manipulation of a high-affinity PHR1 target ciselement to improve phosphorous uptake in Oryza sativa L. Plant Mol Biol 87:429-440
Pubmed: Author and Title
CrossRef: Author and Title
Google Scholar: Author Only Title Only Author and Title

Rubio V, Linhares F, Solano R, Martin AC, Iglesias J, Leyva A, Paz-Ares J (2001) A conserved MYB transcription factor involved in phosphate starvation signaling both in vascular plants and in unicellular algae. Genes Dev 15: 2122-2133
Pubmed: Author and Title
CrossRef: Author and Title
Google Scholar: Author Only Title Only Author and Title

Secco D, Jabnoune M, Walker H, Shou HX, Wu P, Poirier Y, Whelan J (2013) Spatio-Temporal Transcript Pro?ling of Rice Roots and Shoots in Response to Phosphate Starvation and Recovery. Plant Cell 25: 4285-4304
Pubmed: Author and Title
CrossRef: Author and Title
Google Scholar: Author Only Title Only Author and Title

Shin H, Shin HS, Dewbre GR., Harrison MJ (2004) Phosphate transport in Arabidopsis: Pht1;1 and Pht1;4 play a major role in phosphate acquisition from both low- and high-phosphate environments. Plant J 39: 629-642

Pubmed: Author and Title
CrossRef: Author and Title
Google Scholar: Author Only Title Only Author and Title

Tran HT, Qian W, Hurley BA, She YM, Wang D, Plaxton WC (2010) Biochemical and molecular characterization of AtPAP12 and AtPAP26: the predominant purple acid phosphatase isozymes secreted by phosphate-starved Arabidopsis thaliana. Plant Cell Environ 33:1789-1803
Pubmed: Author and Title
CrossRef: Author and Title
Google Scholar: Author Only Title Only Author and Title

Tran HT, Hurley BA & Plaxton WC (2010) Feeding hungry plants: the role of purple acid phosphatases in phosphate nutrition. Plant Sci 179:14-27
Pubmed: Author and Title
CrossRef: Author and Title
Google Scholar: Author Only Title Only Author and Title

Varkonyi-Gasic E, Wu R, Wood M, Walton EF, Hellens RP (2007) Protocol: a highly sensitive RT-PCR method for detection and quantification of microRNAs. Plant Methods 3:12
Pubmed: Author and Title
CrossRef: Author and Title
Google Scholar: Author Only Title Only Author and Title

Wang C, Huang W, Ying Y, Li S, Secco D, Tyerman S, Whelan J, Shou H (2012) Functional characterization of the rice SPX-MFS family reveals a key role of OsSPX-MFS1 in controlling phosphate homeostasis in leaves. New Phytol 196:139-148
Pubmed: Author and Title
CrossRef: Author and Title
Google Scholar: Author Only Title Only Author and Title

Wang J, Sun J, Miao J, Guo J, Shi Z, He M, Chen Y, Zhao X, Li B, Han F, Tong Y, Li Z (2013) A phosphate starvation response regulator Ta-PHR1 is involved in phosphate signalling and increases grain yield in wheat. Ann Bot 111:1139-1153
Pubmed: Author and Title
CrossRef: Author and Title
Google Scholar: Author Only Title Only Author and Title

Wang ZY, Ruan WY, Shi J, Zhang L, Xiang D, Yang C, Li CY, Wu ZC, Liu Y, Yu YN, Shou HX, Mo XR, Mao CZ, Wu P (2014) Rice SPX1 and SPX2 inhibit phosphate starvation responses through interacting with PHR2 in a phosphate-dependent manner. Proc Natl Acad Sci 111: 14953-14958
Pubmed: Author and Title
CrossRef: Author and Title
Google Scholar: Author Only Title Only Author and Title

Wissuwa M (2003) How do plants achieve tolerance to phosphorus deficiency? Small causes with big effects. Plant Physiol 133:1947-1958
Pubmed: Author and Title
CrossRef: Author and Title
Google Scholar: Author Only Title Only Author and Title

Wu P, Shou HX, Xu GH, Lian XM (2013) Improvement of phosphorus ef?ciency in rice on the basis of understanding phosphate signaling and homeostasis. Curr Opin Plant Biol 16:1-8
Pubmed: Author and Title
CrossRef: Author and Title
Google Scholar: Author Only Title Only Author and Title

Yang XJ, Finnegan PM (2010) Regulation of phosphate starvation responses in higher plants. Ann Bot (Lond) 105: 513-526
Pubmed: Author and Title
CrossRef: Author and Title
Google Scholar: Author Only Title Only Author and Title

Yi KK, Wu ZC, Zhou J, Du LMg, Guo LB, Wu YR, Wu P (2005) OsPTF1, a novel transcription factor involved in tolerance to phosphate starvation in rice. Plant Physiol 138:2087-2096
Pubmed: Author and Title
CrossRef: Author and Title
Google Scholar: Author Only Title Only Author and Title

Yu B, Xu C, Benning C (2002) Arabidopsis disrupted in SQD2 encoding sulfolipid synthase is impaired in phosphate-limited growth. Proc Natl Acad Sci 99:5732-5737
Pubmed: Author and Title
CrossRef: Author and Title
Google Scholar: Author Only Title Only Author and Title

Zhang Q, Wang C, Tian J, Li K, Shou H (2011) Identification of rice purple acid phosphatases related to posphate starvation signaling. Plant Biology 13:7-15
Pubmed: Author and Title
CrossRef: Author and Title
Google Scholar: Author Only Title Only Author and Title

Zhang Z, Liao H, Lucas WJ (2014) Molecular mechanisms underlying phosphate sensing, signaling, and adaptation in plants. J Integr Plant Biol. 56:192-220
Pubmed: Author and Title
CrossRef: Author and Title

Zhou J, Jiao F, Wu Z, Li Y, Wang X, He X, Zhong W, Wu P (2008) OsPHR2 is involved in phosphate-starvation signaling and excessive phosphate accumulation in shoots of plants. Plant Physiol 146:1673-1686
Pubmed: Author and Title
CrossRef: Author and Title
Google Scholar: Author Only Title Only Author and Title

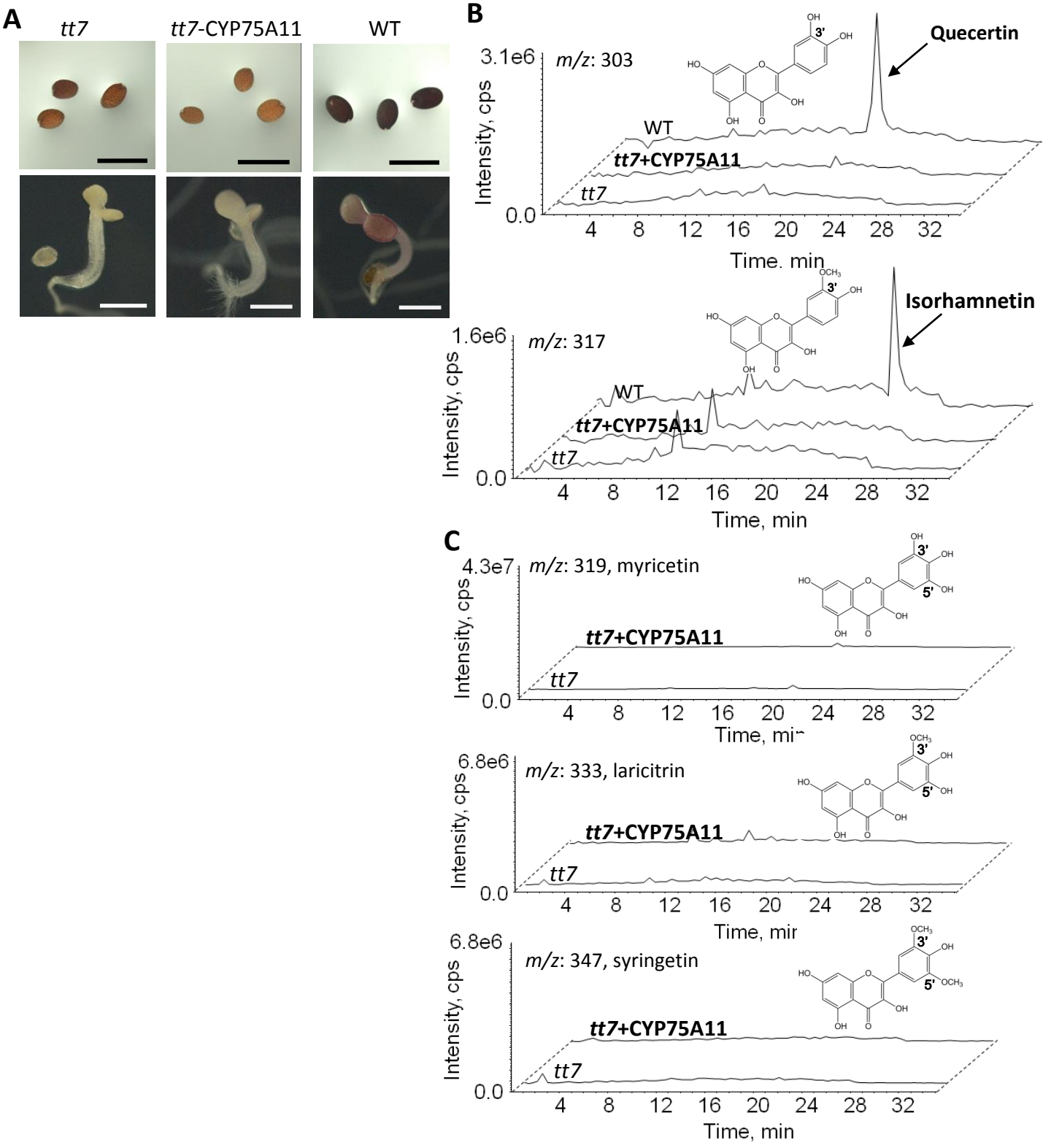

Supplementary Figure S1. Transgenic analysis of CYP75A11 in *Arabidopsis tt7* mutants. A, Expression of CYP75A11 did not restore the accumulation of proanthocyanin in seed coats or red anthocyanin under nitrogen stress in *tt7* mutants. (scale bar = 1 mm). B and C, Expression of CYP75A11 did not result in the accumulation of 3'-and 3', 5'-modified flavonols in transgenic *tt7* plants. LC-MS chromatograms are representatives of at least three independent experiments.

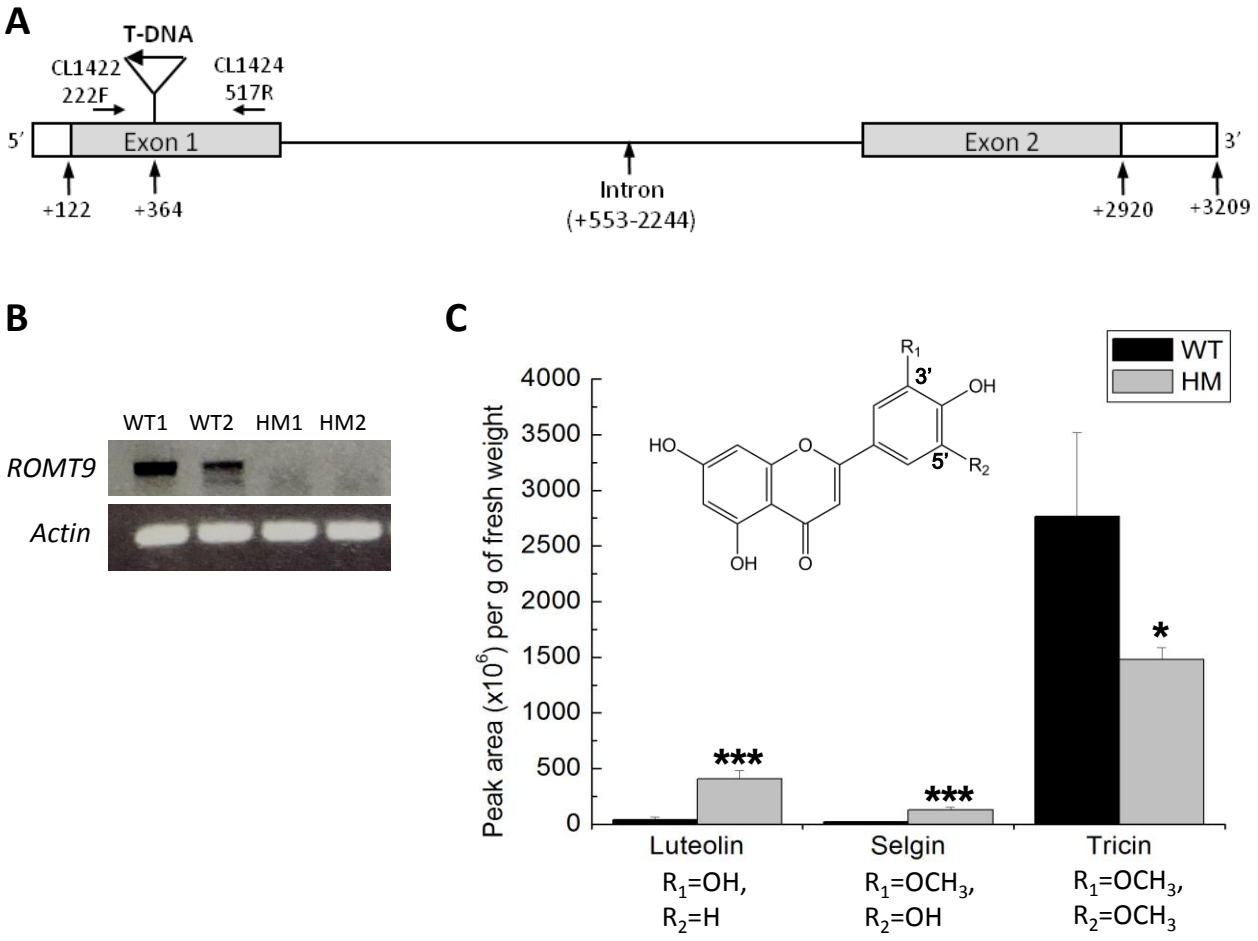

Supplementary Figure S2. Analysis of the rice ROMT9 T-DNA insertion mutant. A, Gene structure of *ROMT9* (*Os08g06100*) and the site of T-DNA insertion in the mutant. B, RT-PCR expression analysis using primers CL1422+CL1424 as indicated in A. C, Relative levels of apigenin, selgin, and tricin in acid-hydrolyzed extracts of HM and WT seedlings as determined by LC-MS. Error bars represent standard deviation (n = 5, *P < 0.05, ***P < 0.001 by Student's *t*-test).

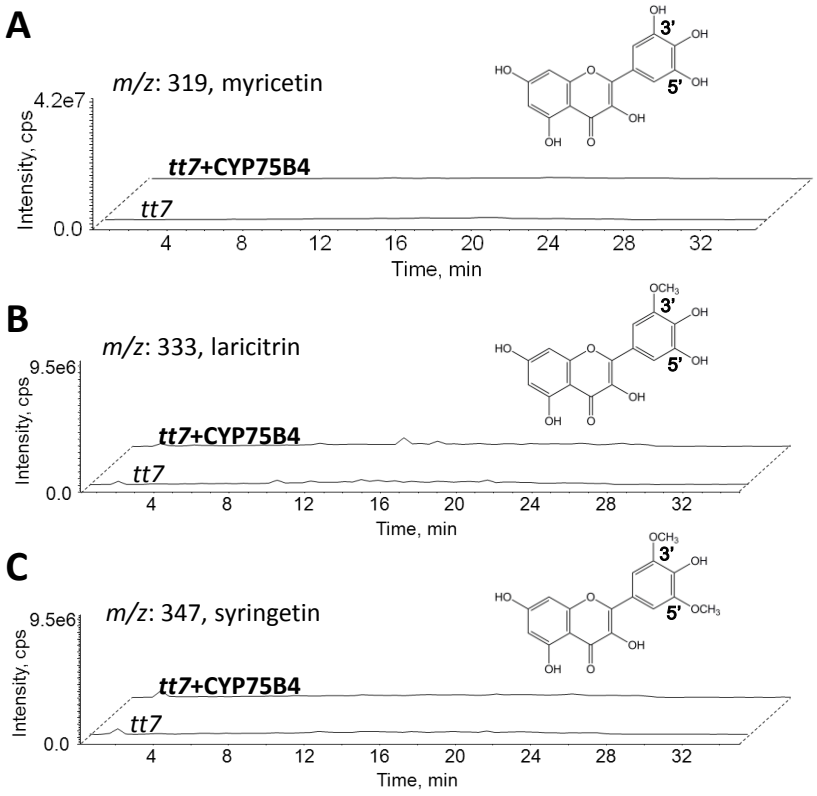

Supplementary Figure S3. LC-MS analysis of 3', 5'-modified flavonols in CYP75B4-expressing *Arabidopsis tt7* mutants. The transgenic *tt7* plants did not accumulate A, myricetin, B, laricitin or C, syringetin. LC-MS chromatograms are representatives of at least three independent experiments.

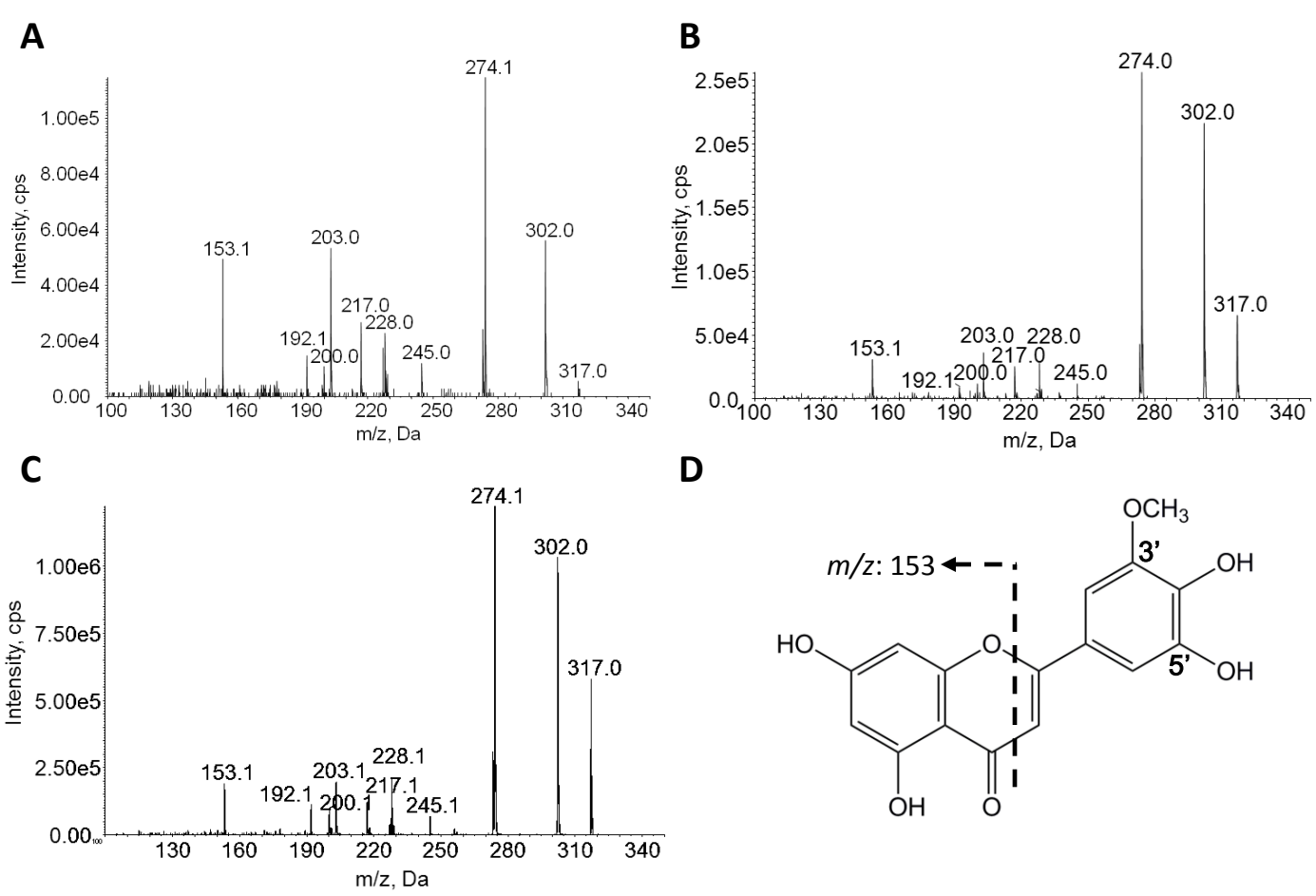

Supplementary Figure S4. Identification of selgin ions (m/z 317) from different sources in this study. MS/MS fragmentation patterns of the major peak at *m/z* 317 detected in A, acid hydrolyzed extracts of CYP75B4 + CYP93G1 co-expressing Arabidopsis plants (Fig. 3C), B, CYP75B4 enzyme assays using chrysoeriol as a substrate (Fig. 4A), and C, selgin generated by the tricetin + ROMT9 reaction (Fig. 4A). D, Structure and fragmentation scheme of selgin. Other major fragments include $[M+H-CH_3-CO]^+$ (*m/z* 274) and $[M+H-CO]^+$ (*m/z* 302).

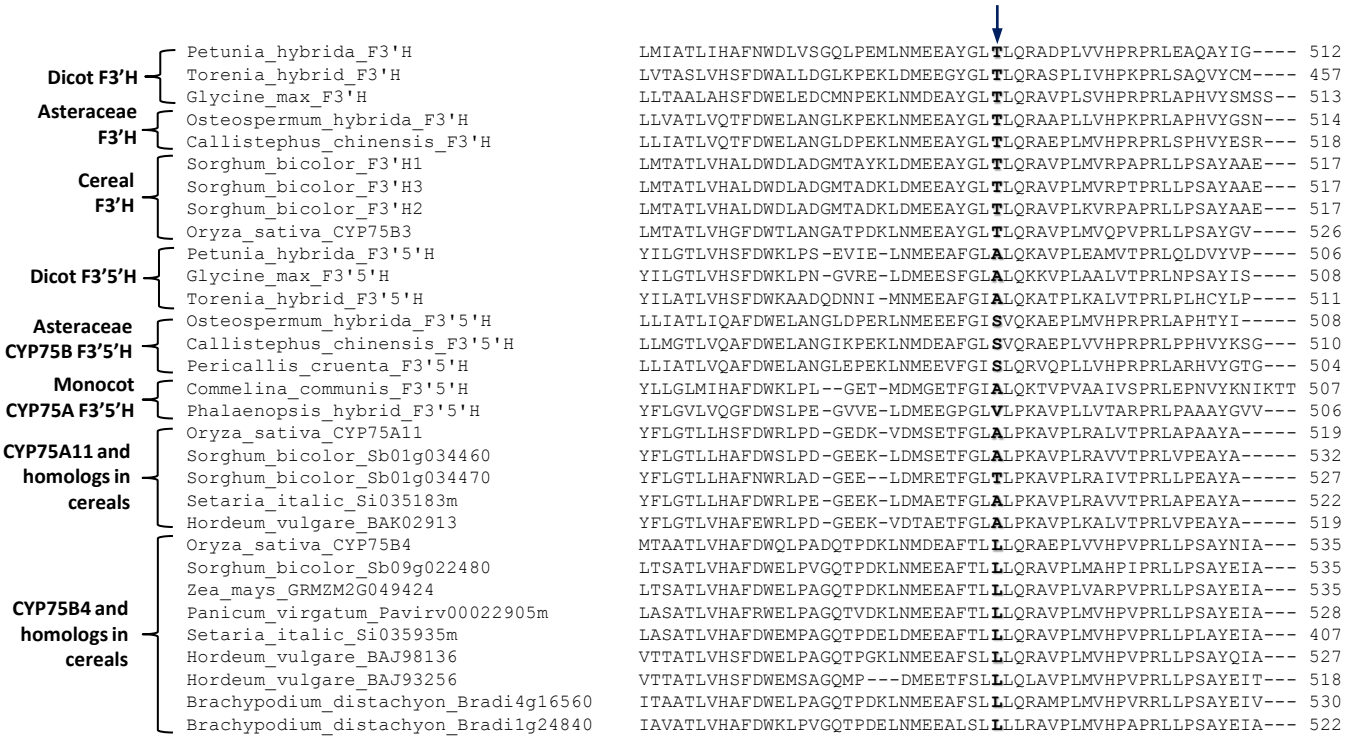

Supplementary Figure S5. Multiple sequence alignment of CYP75A and CYP75B sequences (C-terminal region). The alignment was performed by ClustalW2. The typical Thr of F3'Hs (arrowed) is substituted by Ala in the dicot F3'5'Hs or by Ser in the Asteraceae CYP75B F3'5'H sequences. In CYP75B4 and related sequences, it is replaced by a Thr to Leu substitution.